International Journal of Wavelets, Multiresolution and Information Processing

WAVELET TRANSFORMS GENERATED BY SPLINES

AMIR Z. AVERBUCH
School of Computer Science
Tel Aviv University
Tel Aviv 69978, Israel
amir1@post.tau.ac.il

VALERY A. ZHELUDEV
School of Computer Science
Tel Aviv University
Tel Aviv 69978, Israel
zhel@post.tau.ac.il

Received (Day Month Year)
Revised (Day Month Year)
Communicated by (xxxxxxxxxx)

In this paper we design a new family of biorthogonal wavelet transforms that are based on polynomial and discrete splines. The wavelet transforms are constructed via lifting steps, where the prediction and update filters are derived from various types of interpolatory and quasi-interpolatory splines. The transforms use finite and infinite impulse response (IIR) filters and are implemented in a fast lifting mode. We analyze properties of the generated scaling functions and wavelets. In the case when the prediction filter is derived from a polynomial interpolatory spline of even order the synthesis scaling function and wavelet are splines of the same order. We formulate conditions for the IIR filter to generate an exponentially decaying scaling function.

Keywords: Wavelet, spline, lifting, subdivision, filter.

AMS Subject Classification: 65T60, 42C40, 65D07

1. Introduction

In this paper we describe a new generic technique for the design of biorthogonal wavelet transforms. Some of the results that are presented in this paper have already appeared in [6−9]. However, this paper contains a unified theory that combines a full theoretical justification of the previous results with new facts about the spline-based wavelet transforms. This spline-based technique enables us to construct a wide family of transforms with various properties. It supports flexible adaptation of the transforms to the problems under consideration. In particular, the newly designed transforms prove to be efficient for distinct computational problems such as image compression, feature extraction for signal identification, to name a few.

The performance of the suggested transforms for still image compression is similar to the performance of the transform with 9/7 wavelets ([4]) on most of the benchmark images. Our approach combines custom-design capabilities which are inherent in the lifting schemes [41] with the usage of the well-developed theory of interpolatory, quasi-interpolatory, continuous and discrete splines [32 39 46 47].

Polynomial splines are a common source for wavelet constructions. Until recently, two approaches governed the construction of wavelet schemes that use splines. One is based on orthogonal ([11 26]) and semi-orthogonal wavelets in spline spaces [13 44 48]. This approach produces, in particular, compactly supported spline wavelets. However, their dual wavelets have infinite support. The other approach, which employs splines in wavelet analysis, was introduced by Cohen, Daubechies and Feauveau [14], who constructed symmetric compactly supported spline wavelets whose dual wavelets remain compactly supported and symmetric but do not belong to a spline space.

However, since the introduction of the lifting scheme for the design of wavelet transforms [41], a new way has been opened for the use of splines as a tool for devising wavelet transforms. Main steps of this scheme are an accurate prediction of odd subarray of a signal through the filtered even array and update of the even array using the filtered new odd array in order to smooth the former. The transform generates biorthogonal wavelet bases for the signal space. The structure of the transform and its generated wavelets are determined by the choice of the predicting and updating filters. In the construction by Donoho [21], an odd sample is predicted from a polynomial interpolation of neighboring even samples. We propose to construct a spline, which interpolates or quasi-interpolates even samples of a signal and to use values of this spline at midpoints between the (quasi-)interpolation points as predictions for odd samples of the signal. By using splines of various types and orders we obtain a variety of filters for the *predict* step. After a proper modification, these filters can be used for the *update* step in the lifting scheme. Different combinations of the prediction and update filters that are derived from splines, generate a wide family of biorthogonal symmetric wavelet transforms with diverse properties. In the following we specify how to use different types of splines for the design of filters.

Continuous interpolatory splines: The interpolatory splines of odd order (even degree) are especially suitable for the prediction due to the so-called super-convergence property at the midpoints [46]. To be specific, if a spline of order $p = 2r - 1$ interpolates a polynomial of degree $p = 2r - 1$ on the grid $\{2k\}$ then it predicts exactly the values of the polynomial at points $\{2k + 1\}$.

Discrete interpolatory splines: Another option is to use the discrete interpolatory splines [29]. Discrete splines are functions that are defined on $\mathbb{Z}$, which are the counterparts of polynomial splines. In this case, explicit formulas for the transforms that have any number of vanishing moments are established. Moreover, our investigation reveals an interesting relation between

discrete splines and Butterworth filters, which are commonly used in signal processing [28]. Unlike the construction in [21], the above transforms use pairs of causal-anticausal filters with infinite impulse response (IIR). Fortunately, the transfer functions of the employed filters are rational. Therefore, filtering can be performed recursively.

One-directional causal Butterworth filters were used for devising orthogonal non-symmetric wavelets [25]. A scheme that used recursive filters for the construction of biorthogonal symmetric wavelets and their application to image processing was presented in [27 31].

Quasi-interpolatory splines: The finite impulse response (FIR) filters are more suitable for real-time processing. There is a way to devise wavelet transforms that employ FIR filters whose properties are similar to the properties of the above mentioned interpolatory transforms. It can be done using the so-called local quasi-interpolatory polynomial splines [46]. Like the interpolatory splines, the quasi-interpolatory splines of odd order also possess the super-convergence property.

Parametric splines: Analysis of approximation properties of interpolatory and quasi-interpolatory splines enables us to devise parameterized sets of splines, that are used for the prediction. In particular, specific choices of the parameters result in increasing numbers of vanishing moments.

Lifting implementation of a wavelet transform of a signal is equivalent to processing the signal by a perfect reconstruction filter bank. This filter bank generates analysis and synthesis scaling functions which are solutions for the refinement equations [16]. These scaling functions are constructed via a cascade algorithm, which is closely related to subdivision schemes. We investigate convergence of the cascade algorithm and the regularity of the derived scaling functions and wavelets.

When the filter bank consists of FIR filters, the corresponding scaling functions are compactly supported. This is not the case for IIR filters. We prove that the scaling functions generated by filters with rational transfer functions decay exponentially as their arguments tend to infinity. Obviously this result is not surprising. There are hints to this fact in [15 25]. But the authors never saw a proof of this result. In some sense, a reciprocal fact was established in [17]. Under certain assumptions exponential decay of a refined function implies exponential decay of the refinement mask.

Note that IIR filters with rational transfer functions, which allow recursive implementation, appear in signal processing algorithms using spline functions. Construction and implementation of these filters was studied in [42 43].

The rest of the paper is organized as follows. In the introductory Section 2 we outline the lifting scheme of wavelet transforms and discuss its relation to the conventional setting of wavelet transforms. In Section 3 we establish some necessary properties of polynomial splines and describe the derivation of the prediction filters from interpolatory and local quasi-interpolatory splines. We also construct

parameterized sets of splines and corresponding prediction filters, which have rational and polynomial transfer functions. In Section 4 we design prediction filters using discrete splines and explain the relation of these filters to Butterworth filters. In Section 5 we indicate that slightly updated prediction filters can be employed as update filters. In Section 6 we outline the subdivision scheme, which produces scaling functions and wavelets using IIR filter banks and the properties of these scaling functions and wavelets. In particular, a theorem about the exponential decay of the scaling functions is formulated. We prove that when the prediction filter originates from the polynomial interpolatory splines of even order $2r$, the corresponding synthesis scaling function coincides with the fundamental spline of order $2r$. The super-convergence property implies that the scaling functions derived from splines of odd order are smoother than the splines themselves. In Section 7 we list a number of filters that were derived from splines and, by combining these filters, we construct a number of biorthogonal wavelet transforms. We provide graphical illustrations and summarize the properties of these transforms.

2. Preliminaries: Biorthogonal wavelet transforms

In this section we outline known facts, which are needed for the construction of biorthogonal wavelet transforms.

We call the sequences $\mathbf{x} \triangleq \{x_k\},\ k \in \mathbb{Z}$, which belong to the space l_1, discrete-time signals. The z-transform of a signal $\mathbf{x}$ is defined as $X(z) \triangleq \sum_{k\in\mathbb{Z}} z^{-k}\, x_k$. Throughout the paper we assume that $z = e^{i\omega}$. The input x_n and the output y_n of a linear discrete time shift-invariant system are linked as

$$y_n = \sum_{k\in\mathbb{Z}} f_k x_{n-k}. \tag{2.1}$$

Such a processing of the signal $\mathbf{x}$ is called digital filtering and the sequence $\{f_n\}$ is called the impulse response of the filter $\mathbf{f}$. Its z-transform $F(z) = \sum_{n=-\infty}^{\infty} z^{-n} f_n$ is called the transfer function of the filter. Usually, a filter is designated by its transfer function $F(z)$. Denote by

$$\widehat{X}(\omega) = \sum_{n\in\mathbb{Z}} e^{-i\omega n} x_n, \quad \widehat{Y}(\omega) = \sum_{n\in\mathbb{Z}} e^{-i\omega n} y_n, \quad \widehat{F}(\omega) = \sum_{n\in\mathbb{Z}} e^{-i\omega n} f_n$$

the discrete-time Fourier transforms of the sequences. The function $\widehat{F}(\omega)$ is called the frequency response of the digital filter. Then, we have from (2.1) $Y(z) = F(z)X(z)$, and $\widehat{Y}(\omega) = \widehat{F}(\omega)\widehat{X}(\omega)$.

2.1. *Lifting scheme of the wavelet transform*

We use for the construction and implementation of biorthogonal wavelet transforms the so-called lifting scheme, which was introduced by Sweldens [41].

2.1.1. *Decomposition*

Generally, the primal lifting mode of the wavelet transform consists of four steps: 1. Split. 2. Predict. 3. Update or lifting. 4. Normalization.

Split- The array $\mathbf{x}$ is split into even and odd sub-arrays: $\mathbf{e^1} = \{e_k^1 = x_{2k}\}$, $\mathbf{o^1} = \{o_k^1 = x_{2k+1}\}$, $k \in \mathbb{Z}$.

Predict - The even array $\mathbf{e^1}$ is filtered by some filter $U(z)$, in order for the filtered version of $\mathbf{e^1}$ to predict the odd array $\mathbf{o^1}$. Then, the existing array $\mathbf{o^1}$ is replaced by the array $\mathbf{o_\nu^1}$, which is the difference between $\mathbf{o^1}$ and the predicted array. The filter $U(z)$ is called the *prediction* filter. In the z-domain the operations are described as follows: $O_\nu^1(z) = O^1(z) - U(z)E^1(z)$, where $O_\nu^1(z)$, $O^1(z)$, $E^1(z)$ are the z-transforms of the signals $\mathbf{o_\nu^1}$, $\mathbf{o^1}$, $\mathbf{e^1}$, respectively. From now on the subscript ν designates the new array. We assume that the function $U(z)$ is regular at a certain vicinity of the unit circle $|z| = 1$ including the circle. In addition, we assume that $z^{-1}U(z^2)$ is a real-valued function as $|z| = 1$. In addition, $U(1) = 1$. If the filtered version of $\mathbf{e^1}$ well approximates $\mathbf{o^1}$ then, after this step, the signal is decorrelated.

Update (lifting) - Generally, downsampling the original signal $\mathbf{x}$ into $\mathbf{e^1}$ depletes the smoothness of the signal. To obtain a sparse signal similar to the original $\mathbf{x}$, the new odd array is filtered by an *update* filter, which we prefer to denote $V(z)/2$. The filtered array is used to increase the smoothness of the even array $\mathbf{e^1}$: $E_\nu^1(z) = E^1(z) + \frac{1}{2}V(z)\,O_\nu^1(z)$. The assumption about the filter $V(z)$ is similar to the assumption about U: the function $V(z)$ must be regular at a certain vicinity of the unit circle $|z| = 1$ including the circle and $zV(z^2)$ must be a real-valued function as $|z| = 1$ and $V(1) = 1$. Provided that the filter V is properly chosen, the even array $\mathbf{e^1}$ is transformed into a smoothed and downsampled replica of $\mathbf{x}$.

Normalization - Finally, the smoothed array $\mathbf{s^1}$ and the array of details $\mathbf{d^1}$ are obtained by the following operation: $\mathbf{s^1} = \sqrt{2}\,\mathbf{e_\nu^1}$, $\quad \mathbf{d^1} = \mathbf{o_\nu^1}/\sqrt{2}$.

The key issue in the lifting scheme is the proper choice of the filters U and V. We address this issue in subsequent sections.

2.1.2. *Reconstruction*

One of the most attractive features of lifting schemes is that the reconstruction of the signal $\mathbf{x}$ from the arrays $\mathbf{s^1}$ and $\mathbf{d^1}$ is implemented by the reverse :

Undo Normalization - $\mathbf{e_\nu^1} = \mathbf{s^1}/\sqrt{2} \quad \mathbf{o_\nu^1} = \sqrt{2}\,\mathbf{d^1}$.

Undo Lifting - The even array is restored: $E^1(z) = E_\nu^1(z) - \frac{1}{2}V(z)O_\nu^1(z)$.

Undo Predict - The odd array is restored: $O^1(z) = O_\nu^1(z) + U(z)E^1(z)$

Undo Split - The last step is the standard restoration of the signal from its even and odd components. In the z-domain it appears as: $X(z) = E^1(z^2) + z^{-1}O^1(z^2)$.

2.2. *Filter banks and bases for the signal space*

Let $\Phi(z) \triangleq (1 + z^{-1}U(z^2))/2$ and define the following filters

$$\tilde{G}(z) \triangleq \sqrt{2}z^{-1}\Phi(-z),\ \tilde{H}(z) \triangleq \sqrt{2}(1 + zV(z^2)\Phi(-z)),\ H(z) \triangleq \sqrt{2}\Phi(z),\ G(z) \triangleq z^{-1}\tilde{H}(-z) \quad (2.2)$$

Here $\tilde{H}(z)$ and $\tilde{G}(z)$ are the low- and high-pass analysis filters, respectively, and $H(z)$ and $G(z)$ are the low- and high-pass synthesis filters, respectively. These four filters form a perfect reconstruction filter bank.

Proposition 2.1. *If $z^{-1}U(z^2)$ and $zV(z^2)$ are real valued on the unit circle $z = e^{i\omega}$ then the decomposition and reconstruction equations can be represented as follows:*

$$\begin{aligned} S^1(z^2) &= \tfrac{1}{2}\Big(\overline{\tilde{H}(z)}\,X(z) + \overline{\tilde{H}(-z)}\,X(-z)\Big) \\ D^1(z^2) &= \tfrac{1}{2}\Big(\overline{\tilde{G}(z)}\,X(z) + \overline{\tilde{G}(-z)}\,X(-z)\Big) \end{aligned} \quad (2.3)$$

$$X(z) = H(z)S^1(z^2) + G(z)\,D^1(z^2), \quad (2.4)$$

where $S^1(z)$ and $D^1(z)$ are the z-transforms of the arrays $\mathbf{s^1}$ and $\mathbf{d^1}$, respectively.

In addition, the perfect reconstruction property holds

$$H(z)\,\overline{\tilde{H}(z)} + G(z)\,\overline{\tilde{G}(z)} = 2 \quad H(z)\,\overline{\tilde{H}(-z)} + G(z)\,\overline{\tilde{G}(-z)} = 0. \quad (2.5)$$

The proof of this simple assertion can be found, for example, in [6].

The perfect reconstruction filter banks, described above, are associated with the biorthogonal pairs of bases in the space of discrete-time signals.

The impulse responses of the filters $H(z), G(z), \tilde{H}(z), \tilde{G}(z)$ are $\{h_k\}$, $\{g_k\}$, $\{\widetilde{h}_k\}$, $\{\widetilde{g}_k\}$, $k \in \mathbb{Z}$, respectively. It means, for example, that $H(z) = \sum_{k\in\mathbb{Z}} z^{-k}h_k$. On the other hand, $\mathbf{h} \triangleq \{h_k\}$ is the signal, which emerges as a result of the application of the filter $H(z)$ to the impulse signal δ_n (the Kroneker delta). Similar relations hold for the other functions. The shifts of these impulse response signals form a biorthogonal pair of bases for the signal space.

Proposition 2.2. *Any signal $\mathbf{x} \in l^1$ can be represented as follows: $x_l = \sum_{k\in\mathbb{Z}} s^1_k\,\varphi^1_{l-2k} + \sum_{k\in\mathbb{Z}} d^1_k\,\psi^1_{l-2k}$, where $\varphi^1_k \triangleq h_k$, $\psi_k \triangleq g_k$, $k \in \mathbb{Z}$. The coordinates s^1_k and d^1_k are the following inner products: $s^1_k = \sum_{n\in\mathbb{Z}} \tilde{\varphi}^1_{n-2k}x_n$, $d^1_k = \sum_{n\in\mathbb{Z}} \tilde{\psi}^1_{n-2k}x_n$, where $\widetilde{\varphi}^1_k \triangleq \widetilde{h}_k$, $\widetilde{\psi}^1_k \triangleq \widetilde{g}_k$, $k \in \mathbb{Z}$.*

For the proof we also refer to [6]. Proposition 2.2 justifies the following definition.

Definition 2.1. *The discrete-time signals $\varphi^1 \triangleq \{\varphi^1_k\}$ and $\psi^1 \triangleq \{\psi^1_k\}$, $k \in \mathbb{Z}$, are called the low- and high-frequency synthesis discrete-time wavelets of the first scale, respectively. The signals $\tilde{\varphi}^1 \triangleq \{\tilde{\varphi}^1_k\}$ and $\tilde{\psi}^1 \triangleq \{\tilde{\psi}^1_k\}$, $k \in \mathbb{Z}$ are called the low- and high-frequency analysis discrete-time wavelets of the first scale, respectively.*

The perfect reconstruction property (2.5) implies the following biorthogonal relations:

$$\sum_{n\in\mathbb{Z}} \tilde{\varphi}^1_{n-2k}\,\varphi^1_{n-2l} = \sum_{n\in\mathbb{Z}} \psi^1_{n-2k}\,\tilde{\psi}^1_{n-2l} = \delta^l_k,$$
$$\sum_{n\in\mathbb{Z}} \tilde{\varphi}^1_{n-2k}\,\psi^1_{n-2l} = \sum_{n\in\mathbb{Z}} \tilde{\psi}^1_{n-2l}\,\varphi^1_{n-2k} = 0,\ \forall l,\ k.$$

We say that a discrete-time wavelet ψ has m vanishing moments if the following relations hold: $\sum_{k\in\mathbb{Z}} k^s\psi_k = 0, \quad s = 0, 1, \ldots, m-1.$

Proposition 2.3. *Let the transfer functions $U(z)$ and $V(z)$, which are used for the* predict *and* update *steps, respectively, be rational. If $1 + z^{-1}U(z^2) = (z + 2 + z^{-1})^r\rho(z)$ and $\rho(z)$ has no poles on the unit circle $|z| = 1$ then the high-frequency analysis wavelet $\tilde{\psi}^1$ has $2r$ vanishing moments. If the above condition is satisfied and, in addition, $1 + zV(z^2) = (z + 2 + z^{-1})^p\varrho(z)$ and $\varrho(z)$ has no poles on the unit circle then the high-frequency synthesis wavelet ψ^1 has $2s$ vanishing moments, where $s = \min(p, r)$.*

Proof. Let us ignore for a moment the assumption $|z| = 1$ and examine the function $\tilde{q}(z) \triangleq \tilde{G}(z^{-1}) = \sum_{k\in\mathbb{Z}} z^k\tilde{\psi}^1_k$ of the complex variable z. We have $\tilde{q}(z) = z^{-1}(1 - zU(z^{-2}))/\sqrt{2} = (1-z)^{2r}\,\widetilde{Q}(z)$, where $\widetilde{Q}(z)$ is a regular function at the vicinity of $z = 1$. It is clear that $\tilde{q}^{(s)}(1) = 0,\ s = 0, 1, \ldots, 2r-1$. On the other hand, $\tilde{q}^{(s)}(1) = \sum_{k\in\mathbb{Z}} k^{[s]}\tilde{\psi}^1_k$, where $k^{[s]} \triangleq k(k-1)(k-2)\cdots(k-s+1)$. Note that any monomial k^l can be represented as a linear combination of the polynomials $k^{[n]},\ n = 0, \ldots, l$. Thus, the wavelet $\tilde{\psi}^1$ has $2r$ vanishing moments. Denote $q(z) \triangleq G(z^{-1}) = \sum_{k\in\mathbb{Z}} z^k\psi^1_k$. If $1 - zV(z^2)$ comprises the factor $(z - 2 + z^{-1})^p$ then we have

$$\begin{aligned} q(z) &= z\sqrt{2}\left(1 - (2z)^{-1}V(z^{-2})(1 + zU(z^{-2}))\right) \\ &= \frac{z}{\sqrt{2}}\left((1 - z^{-1}V(z^{-2})) + (1 - zU(z^{-2})) + zU(z^{-2})(1 - z^{-1}V(z^{-2}))\right) \\ &= (1-z)^{2s}\,Q(z), \end{aligned}$$

where $s = \min(p, r)$ and $Q(z)$ is a regular function in the vicinity of $z = 1$. Thus, the wavelet ψ^1 has $2s$ vanishing moments. □

Expansion of the transform to coarser scales is implemented in a recursive way.

The discrete-time wavelets related to the subsequent scales are defined iteratively via the two-scale equations

$$\varphi^{j+1}_l \triangleq \sum_{k\in\mathbb{Z}} h_k\varphi^j_{l-2k}, \quad \psi^{j+1}_l \triangleq \sum_{k\in\mathbb{Z}} g_k\varphi^j_{l-2k},$$
$$\widetilde{\varphi}^{j+1}_l \triangleq \sum_{k\in\mathbb{Z}} \widetilde{h}_k\widetilde{\varphi}^j_{l-2k}, \quad \widetilde{\psi}^{j+1}_l \triangleq \sum_{k\in\mathbb{Z}} \widetilde{g}_k\widetilde{\varphi}^j_{l-2k}.$$

3. Design of prediction filters using polynomial splines

We derive the prediction filters from splines in the following way: We construct a spline, which interpolates or quasi-interpolates even samples of a signal and predict odd samples as the values of the spline calculated at the midpoints between the points of (quasi-)interpolation. Analytically, this operation reduces to filtering the even array. We will show that splines of odd order are more suitable for this design due to the property of superconvergence of splines of odd order at the midpoints.

3.1. *B-splines*

We outline here some known properties of B-splines and establish a few facts needed for our constructions. The centered B-spline of first order is the characteristic function of the interval $[-1/2, 1/2]$. The centered B-spline of order p is the convolution $M^p(x) = M^{p-1}(x) * M^1(x) \quad p \geq 2$. Note that the B-spline of order p is supported on the interval $(-p/2, p/2)$. It is positive within its support and symmetric about zero. The B-spline M^p consists of pieces of polynomials of degree $p-1$ that are linked to each other at the nodes such that $M^p \in C^{p-2}$. Nodes of B-splines of even order are located at points $\{k\}$ and of odd order, at points $\{k+1/2\},\ k \in \mathbb{Z}$. The Fourier transform of the B-spline of order p is

$$\widehat{M^p}(\omega) \triangleq \int_{-\infty}^{\infty} e^{-i\omega x} M^p(x)\, dx = \left(\frac{\sin \omega/2}{\omega/2}\right)^p. \tag{3.1}$$

We introduce two sequences which are important for further construction:

$$\mathbf{u}^p \triangleq \{M^p(k)\}, \quad \mathbf{w}^p \triangleq \left\{ M^p\left(k+\frac{1}{2}\right)\right\},\ k \in \mathbb{Z}. \tag{3.2}$$

Due to the compact support of B-splines, these sequences are finite and symmetric. The discrete-time Fourier transforms of these sequences are

$$\begin{aligned} \widehat{u^p}(\omega) &\triangleq \textstyle\sum_{k=-\infty}^{\infty} e^{-i\omega k} M^p(k) = P^p\left(\cos\tfrac{\omega}{2}\right), \\ \widehat{w^p}(\omega) &\triangleq \textstyle\sum_{k=-\infty}^{\infty} e^{-i\omega k} M^p\left(k+\tfrac{1}{2}\right) = e^{i\omega/2} Q^p\left(\cos\tfrac{\omega}{2}\right). \end{aligned} \tag{3.3}$$

Here the functions P^p and Q^p are real-valued polynomials. If $p = 2r-1$ then P^p is a polynomial of degree $2r-2$ and Q^p is a polynomial of degree $2r-3$. If $p = 2r$ then P^p is a polynomial of degree $2r-2$ and Q^p is a polynomial of degree $2r-1$. These polynomials were extensively studied in [35] [37]. In particular the recurrence relations for their computation were established.

The z-transform s of the sequences $\mathbf{u}^p$ and $\mathbf{w}^p$

$$u^p(z) = \sum_{k=-\infty}^{\infty} z^{-k} M^p(k), \quad w^p(z) = \sum_{k=-\infty}^{\infty} z^{-k} M^p(k+1/2), \tag{3.4}$$

are the so-called Euler-Frobenius polynomials [37].

Proposition 3.1 ([37]). *On the circle $z = e^{i\omega}$ the Laurent polynomials $u^p(z)$ are strictly positive. Their roots are all simple and negative. Each root γ can be paired*

with a dual root $\widetilde{\gamma}$ *such that* $\gamma\,\widetilde{\gamma}=1$. *Thus, if* $p=2r-1$, $p=2r$ *then* $u^p(z)$ *can be represented as follows:*

$$u^p(z)=\prod_{n=1}^{r-1}\frac{1}{\gamma_n}(1+\gamma_n z)(1+\gamma_n z^{-1}),\ \ 0<\gamma_1<\gamma_1<\ldots<\gamma_{r-1}<1. \tag{3.5}$$

3.2. *Euler-Frobenius polynomials and their ratios*

The following facts are needed to establish the approximation order of the forthcoming spline based scaling functions and vanishing moment properties of the corresponding wavelets. Using (3.1) we can write

$$M^p(x-k)=\frac{1}{2\pi}\int_{-\infty}^{\infty}e^{i\omega(x-k)}\left(\frac{\sin\omega/2}{\omega/2}\right)^p d\omega$$
$$=\sum_{l=-\infty}^{\infty}e^{2\pi ilx}\int_0^1 e^{2\pi i\xi(x-k)}\frac{(\sin\pi\xi)^p(-1)^{lp}}{\pi(l+\xi))^p}\,d\xi=\int_0^1 e^{-2\pi i\xi k}m_x^p(\xi)\,d\xi,$$

$$\text{where } m_x^p(\xi)\triangleq e^{2\pi i\xi x}(\sin\pi\xi)^p\sum_{l=-\infty}^{\infty}e^{2\pi ilx}\frac{(-1)^{lp}}{(\pi(l+\xi))^p}. \tag{3.6}$$

Relation (3.6) means that $M^p(x-k)$ is a Fourier coefficient of the 1-periodic function $m_x^p(\xi)$ and this function can be represented as the sum:

$$m_x^p(\xi)=\sum_{k=-\infty}^{\infty}e^{-2\pi ik\xi}\,M^p(x+k). \tag{3.7}$$

Equations (3.3) and (3.7) imply the following representations:

$$P^p(\cos\omega/2)=\widehat{u^p}(\omega)=m_0^p(\omega/2\pi)=(\sin\omega/2)^p\sum_{l=-\infty}^{\infty}\frac{(-1)^{lp}}{(\pi l+\omega/2)^p} \tag{3.8}$$

$$Q^p(\cos\omega/2)=e^{-i\omega/2}\widehat{w^p}(\omega)=e^{-i\omega/2}m_{\frac{1}{2}}^p(\omega/2\pi)=(\sin\omega/2)^p\sum_{l=-\infty}^{\infty}\frac{(-1)^{l(p+1)}}{(\pi l+\omega/2)^p}.$$

It is obvious from (3.8) that

$$P^p(1)=Q^p(1)=1. \tag{3.9}$$

We also introduce two rational functions:

$$R^p(y)\triangleq\frac{Q^p(y)}{P^p(y)},\quad U_i^p(z)\triangleq\frac{w^p(z)}{u^p(z)}. \tag{3.10}$$

The function $U_i^p(z)$ will be used as the prediction filter. Obviously,

$$U_i^p(e^{i\omega})=e^{i\omega/2}\,R^p\left(\cos\frac{\omega}{2}\right),\quad 1+z^{-1}U_i^p(z^2)=1+R^p\left(\frac{z+z^{-1}}{2}\right). \tag{3.11}$$

Examples:

Quadratic spline: $p = 3$

$$U_i^3(z) = 4\frac{1+z}{z+6+z^{-1}}, \quad 1 + z^{-1}U_i^3(z^2) = \frac{(z+2+z^{-1})^2}{z^{-2}+6+z^2}. \quad (3.12)$$

Cubic spline: $p = 4$

$$U_i^4(z) = \frac{(z+1)(z^{-1}+22+z)}{8(z+4+z^{-1})}, \quad (3.13)$$

$$1 + z^{-1}U_i^4(z^2) = \frac{(z^{-1}+2+z)^2(z+4+z^{-1})}{8(z^{-2}+4+z^2)}.$$

Spline of fourth degree: $p = 5$

$$U_i^5(z) = \frac{16(z+10+z^{-1})(1+z)}{z^2+76z+230+76z^{-1}+z^{-2}}, \quad (3.14)$$

$$1 + \frac{U_i^5(z^2)}{z} = \frac{(z+2+z^{-1})^3\,(z+z^{-1}+10)}{z^4+76z^2+230+76z^{-2}+z^{-4}}.$$

One can observe that the filters $1 + z^{-1}U_i^{2r-1}(z^2),\ r = 2, 3$ originated from the splines of second and fourth degrees, comprise the factors $(z+2+z^{-1})^r$. We show that this factorization is common to splines of even degrees and results in the so called super-convergence property, which is valuable for wavelet construction.

The following proposition is proved in [49].

Proposition 3.2 ([49]). *If $p = 2r-1$ then the following factorization formula holds*

$$1 + z^{-1}U_i^{2r-1}(z^2) = (z+2+z^{-1})^r\left(A_r + (z-2+z^{-1})\frac{q(z+2+z^{-1})}{u^{2r-1}(z^2)}\right) \quad (3.15)$$

where

$$A_r \triangleq \frac{(4^r-1)}{r(2r-2)!}|b_{2r}|, \quad (3.16)$$

b_s is the Bernoulli number of order s and q is a polynomial of degree $r-2$.

We conclude the section by a fact about splines of even order.

Proposition 3.3. *If $p = 2r$ then*

$$1 + R^{2r}(\cos\omega/2) = \frac{2(\cos\omega/4)^{2r}P^{2r}(\cos\omega/4)}{P^{2r}(\cos\omega/2)} \quad (3.17)$$

$$1 + z^{-1}U_i^{2r}(z^2) = \frac{(z+2+z^{-1})^r u^{2r}(z)}{2^{2r-1}u^{2r}(z^2)}. \quad (3.18)$$

Proof. From (3.8) and (3.9) we have

$$1 + R^{2r}(\cos\omega/2) = 1 + \frac{Q^{2r}(\cos\omega/2)}{P^{2r}(\cos\omega/2)} = \frac{2(\sin\omega/2)^{2r}\sum_{l=-\infty}^{\infty}(\pi 2l+\omega/2)^{-2r}}{P^{2r}(\cos\omega/2)}$$

$$= \frac{2(\cos\omega/4)^{2r}(\sin\omega/4)^{2r}\sum_{l=-\infty}^{\infty}(\pi l+\omega/4)^{-2r}}{P^{2r}(\cos\omega/2)} = \frac{2(\cos\omega/4)^{2r}P^{2r}(\cos\omega/4)}{P^{2r}(\cos\omega/2)}$$

Equations (3.18) follow immediately from the definition (3.10) and Eq. (3.17). □

3.3. *Filters derived from interpolatory polynomial splines*

Recall that for devising a prediction filter we have to construct the interpolatory spline and calculate its values at the midpoints between the points of interpolation. We do it in this section. We also evaluate the approximation error at the midpoints and prove the super-convergence property.

Shifts of B-splines form a basis in the space of splines of order p on the grid $\{2k\}$. Namely, any spline S^p has the following representation:

$$S^p(x) = \sum_l t_l \, M^p(x/2 - l). \tag{3.19}$$

Denote $\mathbf{t} \triangleq \{t_l\}$ and let $T(z)$ be the z-transform of $\mathbf{t}$. We also introduce the sequences $\mathbf{s}_e^p \triangleq \{s_{e,k}^p \triangleq S^p(2k)\}$, $\mathbf{s}_o^p \triangleq \{s_{o,k}^p \triangleq S^p(2k+1)\}$ and $\mathbf{s}^p = \{s_k^p \triangleq S^p(k)\}$ of values of the spline at

the grid points, at the midpoints and on the whole set $\mathbb{Z}$. The z-transform of the sequence $\mathbf{s}^p$ is

$$s^p(z) = s_e^p(z^2) + z^{-1} s_o^p(z^2). \tag{3.20}$$

We have $s_{e,k}^p = \sum_l t_l \, M^p(k-l)$, $\quad s_{o,k}^p = \sum_l t_l \, M^p\left(k - l + 1/2\right)$. Thus, $s_e^p(z) = T(z)u^p(z)$ and $s_o^p(z) = T(z)w^p(z)$, where $u^p(z)$ and $w^p(z)$ are the functions defined in (3.4). From these formulas we can derive expressions for the coefficients of a spline S_i^p which interpolates a given sequence $\mathbf{e} \triangleq \{e_k\} \in l^1$ at grid points:

$$\begin{aligned} &S_i^p(2k) = e_k, \; k \in \mathbb{Z}, \Longleftrightarrow T(z)u^p(z) = e(z) \Longleftrightarrow T(z) = e(z)/u^p(z) \\ &\Longleftrightarrow t_l = \textstyle\sum_{n=-\infty}^{\infty} \lambda^p(l-n)e(n), \end{aligned} \tag{3.21}$$

where $\lambda^p \triangleq \{\lambda_k^p\}$ is the sequence which is defined via its $z-$transform:

$$\lambda^p(z) = \sum_{k=-\infty}^{\infty} z^{-k} \lambda_k^p = \frac{1}{u^p(z)}. \tag{3.22}$$

It follows immediately from (3.5) that the coefficients $\{\lambda_k^p\}$ decay exponentially as $|k| \to \infty$. We will prove a general statement about this fact in forthcoming Proposition 6.2. Substitution of (3.21) into (3.19) results in an alternative representation of the interpolatory spline:

$$S_i^p(x) = \sum_{l=-\infty}^{\infty} e_l \, L^p(x/2 - l), \qquad \text{where } L^p(x) \triangleq \sum_l \lambda_l^p \, M^p(x - l). \tag{3.23}$$

The spline $L^p(x)$ defined in (3.23) is called the fundamental spline. It interpolates the Kroneker delta sequence δ_k, i.e. it vanishes at all the integer points except $x = 0$, where $L^p(0) = 1$. Because of decaying the coefficients $\{\lambda_k^p\}$, the spline $L^p(x)$ decays exponentially as $|x| \to \infty$. Therefore, the representation (3.23) of the interpolatory

spline remains valid for the sequences $\{e_k\}$, which may grow no faster than a power of k [38]. The values of the fundamental spline at midpoints are

$$L^p\left(k+\frac{1}{2}\right)=\sum_{l\in\mathbb{Z}}\lambda_l^p\,M^p\left(k-l+\frac{1}{2}\right),\quad \sum_{k\in\mathbb{Z}}z^{-k}L^p\left(k+\frac{1}{2}\right)=U_i^p(z),\quad (3.24)$$

where $U_i^p(z)$ is defined in (3.10). Then, we obtain from Eqs. (3.22) and (3.24) that the values of the interpolatory spline at the midpoints are

$$s_{o,k}^p=\sum_n L^p\left(k+\frac{1}{2}-n\right)e_n \Longleftrightarrow s_o^p(z)=U_i^p(z)e(z). \quad (3.25)$$

Switching into the signal processing terminology, we say that, in order to derive the values of the interpolatory spline at the midpoints $\{2k+1\}$ between the points $\{2k\}$ of interpolation, we have to filter the data $\{e_k\}$ by the filter U_i^p whose impulse response $\{L^p\,(k+1/2)\},\ k\in\mathbb{Z}$ is infinite but decays exponentially as $|k|\to\infty$ (IIR filter). As we mentioned above, if a spline ıes even samples of a signal, the values of the spline at the midpoints are used as a prediction of the odd samples of the signal. Thus, the filters U_i^p may serve as prediction filters in the lifting scheme of a wavelet transform.

Combining the results of Proposition 3.2 and Proposition 2.3, we come to the following statement.

Proposition 3.4. *If the filter U_i^p is used as a prediction filter in the lifting scheme then, either by $p=2r-1$ or by $p=2r$, the high-frequency analysis wavelet $\tilde{\psi}^1$ has $2r$ vanishing moments.*

Super-convergence property. Proposition 3.2 implies the super-convergence property of the interpolatory splines of odd order (even degree). Recall, that in general the interpolatory spline of order p (degree $p-1$), which interpolates the values of a polynomial of degree not exceeding $p-1$, coincides with this polynomial (in other words, the spline is exact on polynomials of degree not exceeding $p-1$). However, we will show that the spline S_i^{2r-1} of odd order $2r-1$ (degree $2r-2$), which interpolates the values of a polynomial of degree $2r-1$ on the grid $\{2k\}$ restores the values of this polynomial at the mid-points $\{2k+1\}$ between the grid points. Therefore, we claim that $\{2k+1\}$ are points of super-convergence of the spline S_i^{2r-1}. This property results in the vanishing moments property of the wavelets constructed using the filters U_i^{2r-1}.

Theorem 3.1. *Let a spline S_i^{2r-1} of order $2r-1$ interpolate $f(x)$ on the grid $\{2k\}$. If the function f is a polynomial of degree $2r-1$ then*
$S_i^{2r-1}\,(2k+1)=f\,(2k+1)\ \forall k\in\mathbb{Z}$. *If f is a polynomial of degree $2r+1$ then*

$$S_i^{2r-1}\,(2k+1)=f\,(2k+1)-A_r f^{(2r)}(2k+1). \quad (3.26)$$

The constant A_r is defined in (3.16).

The proof is presented in [49]. Originally this property was proved differently in [46].

It can be easily derived from (3.18) that the splines of order $2r$ restore only polynomials of degree $2r-1$ at the midpoints between the points of interpolation.

Remark: Due to the super-convergence property of the splines of odd order, the wavelets originating from the interpolatory splines of odd order $2r-1$ and of even order $2r$ have the same number of vanishing moments. But the structure of the filter U_i^{2r-1} is simpler than the structure of the filter U_i^{2r} (compare, for example, $U_i^3(z)$ in (3.12) with $U_i^4(z)$ in (3.13)). This means that the computational cost of implementation of the wavelet transform with the filter U_i^{2r-1} is lower than with the filter U_i^{2r}. Moreover, the wavelets originating from U_i^{2r-1} are better localized in time domain. Therefore, for most applications it is preferable to use filters derived from the odd-order splines.

3.4. *Local quasi-interpolatory splines*

We can see from Eq. (3.25) that in order to find the values at the midpoints of the spline that interpolates the array $\mathbf{e}$, the array has to be filtered with the filter whose transfer function is the rational function $U_i^p(z)$. This filter has infinite impulse response (IIR). However, a fast implementation of this operation is possible via the subsequent application of causal and anticausal recursive filtering to $\mathbf{e}$. The procedure is described in [6]. But this procedure can not be used in real-time processing. Also such filtering is not appropriate when the length of a signal to be processed is large. In these situations finite impulse response (FIR) filters are better suited. In this section we describe the construction of FIR prediction filters on the base of the so-called local quasi-interpolatory (LQI) splines. Their properties are similar to the properties of filters derived from interpolatory splines. Even the property of super-convergence at midpoints remains valid for the quasi-interpolatory splines of odd order.

Definition 3.1. *Let a function f be sampled on the grid $\{k\}$, $\mathbf{f} \triangleq \{f_k\}$, and $F(z)$ be the z-transform of $\mathbf{f}$. A spline S^p of order p represented in the form (3.19) is called local if the array $\mathbf{q}$ of its coefficients is derived by FIR filtering of the array $\mathbf{f}$: $T(z) = \Gamma(z)F(z)$, where $\Gamma(z)$ is a Laurent polynomial. The local spline of order p is called quasi-interpolatory (LQI) if it is exact on polynomials of degree not exceeding $p-1$.*

It means that if f is a polynomial of degree $p-1$, then the spline $S^p(x) \equiv f(x)$.

To predict the odd samples we use the values at the midpoints of the splines, which quasi-interpolate the even samples. If $\mathbf{w}^p$ is the sequence defined in (3.4) then the FIR prediction filter, which stems from an LQI spline of order p, is

$$U_q^p(z) \triangleq \Gamma(z) w^p(z). \tag{3.27}$$

Explicit formulas for the construction of quasi-interpolatory splines were given in [35]. Properties of quasi-interpolatory splines and, in particular, their approximation accuracy were studied in [46]. In this work we are interested in splines of odd order $p = 2r - 1$. There are many FIR filters, which generate quasi-interpolatory splines, but for each order $p = 2r - 1$ there is only one filter whose impulse response has minimal length $2r - 1$.

Proposition 3.5 ([35]). *An LQI spline of order $p = 2r - 1$ can be produced by filtering $T(z) = \Gamma(z)F(z)$, with filters Γ of length no less than $2r - 1$. There exists a unique filter Γ_m whose impulse response is of length $2r - 1$, which produces the minimal quasi-interpolatory spline $\tilde{S}_m^{2r-1}(x)$. Its transfer function is:*

$$\Gamma_m(z) = 1 + \sum_{k=1}^{r-1} \beta_k^{2r-1} \, (z^{-1} - 2 + z)^k, \tag{3.28}$$

where the coefficients β_k^{2r-1} are derived from the relation $\left(2t^{-1} \arcsin t/2\right)^p = \sum_{k=0}^{\infty} (-1)^k \beta_k^p t^{2k}$.

Proposition 3.6 ([46]). *If f is a polynomial of degree $2r$ and $\mathbf{f} \triangleq \{f(2k)\}$ then the following relation holds for the minimal quasi-interpolatory spline S_m^{2r-1} of order $2r - 1$ (degree $2r - 2$) for $t = (2k + 1 + \tau)$, $\tau \in [0, 1]$:*

$$S_m^{2r-1}(t) = f(t) - 2^{2r-1} f^{(2r-1)}(t) \frac{b_{2r-1}(\tau)}{(2r-1)!} + 2^{2r} f^{(2r)(t)} \cdot \left(\frac{(2r-1) b_{2r}(\tau)}{(2r)!} - \beta_r^{2r-1} \right),$$

where $b_s(\tau)$ is the Bernoulli polynomial of degree s.

We recall that the values $b_s \triangleq b_s(0)$ are called the Bernoulli numbers [1]. If $s > 1$ is odd then $b_s = 0$. Hence, we obtain the super-convergence property, which is similar to the property of interpolatory splines of odd order.

Corollary 3.1. *If f is a polynomial of degree $2r - 1$, $\mathbf{f} \triangleq \{f(2k)\}$ and S_m^{2r-1} is a minimal LQI spline of order $2r - 1$ (degree $2r - 2$) then $S_m^{2r-1}(2k + 1) \equiv f(2k + 1)$, $k \in \mathbb{Z}$. If f is a polynomial of degree $2r$ then*

$$\begin{gathered} S_m^{2r-1}(2k+1) = f(2k+1) + 2^{2r} f^{(2r)}(2k+1) B_{2r-1}, \\ B_{2r-1} \triangleq (2r-1) b_{2r}/(2r)! - \beta_r^{2r-1}. \end{gathered} \tag{3.29}$$

3.5. *Parametric splines*

3.5.1. *Upgrade of LQI splines*

The representation (3.29) provides tools for custom design of predicting splines that retain or even enhance the approximation accuracy of the minimal LQI spline at the midpoints. This is achieved via an upgrade of the filter Γ_m.

Proposition 3.7. *Let f be a polynomial of degree $2r - 1$, ρ be a real number and $\mathbf{f} \triangleq \{f(2k)\}$. If the coefficients of a spline S_ρ^{2r-1} of order $2r - 1$ are derived from*

the relation $T(z) = \Gamma(z)F(z)$, *with the filter* Γ_ρ *of length* $2r+1$ *with the transfer function* $\Gamma_\rho(z) = \Gamma_m(z) + \rho(z^{-1} - 2 + z)^r$ *then* $S_\rho^{2r-1}(2k+1) \equiv f(2k+1)$, $k \in \mathbb{Z}$ *by any real* ρ. *However, if* $\rho = -B_{2r-1}$ *then the identity* $S_\rho^{2r-1}(2k+1) \equiv f(2k+1)$ *remains valid when* f *is a polynomial of degree* $2r$.

Proof. The spline S_ρ^{2r-1}, which is constructed using the filter Γ_ρ, can be represented by the sum:

$$S_\rho^{2r-1} = S_m^{2r-1} + \rho S_d^{2r-1}, \quad S_d^{2r-1}(t) \triangleq \sum_{l\in\mathbb{Z}} (\mathbf{D}^{2r} f(2l))\, M^{2r-1}(t/2 - l).$$

We evaluate the spline S_d^{2r-1} using the well-known asymptotic relation for a function $\phi \in C^3$ ([36]):

$$\sum_l \phi(hl)\, M^p(t/h - l) = \phi(t) + \frac{ph^2\phi^{''}(t)}{24} + O(h^3\phi^{(3)}).$$

Hence, if f is a polynomial of degree $2r$ then we have $S_d^{2r-1}(t) = \mathbf{D}^{2r} f = 2^{2r} f^{(2r)}$ and

$$S_\rho^{2r-1}(t) = f(t) - 2^{2r-1} f^{(2r-1)}(t) \frac{b_{2r-1}(\tau)}{(2r-1)!} + 2^{2r} f^{(2r)} \left(\frac{(2r-1)b_{2r}(\tau)}{(2r)!} - \beta_r^{2r-1} + \rho \right),$$

At midpoints we have $S_m^{2r-1}(2k+1) = f(2k+1) + 2^{2r} f^{(2r)} \cdot (B_{2r-1} + \rho)$. This equation proves the proposition. □

If the parameter ρ is chosen such that $\rho = (-1)^{r-1}|\rho|$ then the spline S_ρ^{2r-1} possesses the smoothing property [47]. In the case when $\rho = -B_{2r-1}$ we call the spline the extended LQI spline and denote it as S_e^{2r-1}.

We recall that, given a filter $\Gamma(z)$, the prediction filter is derived from Eq. (3.27).

Examples:

Minimal LQI quadratic spline: The filters are

$$\Gamma_m(z) = 1 - \frac{z^{-1} - 2 + z}{8}, \quad U_m^3(z) = \frac{-z^{-1} + 9 + 9z - z^2}{16}, \quad (3.30)$$
$$1 + z^{-1} U_m^3(z^2) = \frac{(z^{-1} + 2 + z)^2 (z^{-1} + 4 + z)}{16}.$$

The corresponding analysis wavelet has four vanishing moments.

Extended LQI quadratic spline:

$$\Gamma_e(z) = \Gamma_m(z) + \frac{3}{128}(z^{-1} - 2 + z)^2,$$
$$U_e^3(z) = \frac{3z^{-2} - 25z^{-1} + 150 + 150z - 25z^2 + 3z^3}{256},$$

$$1 + z^{-1} U_e^3(z^2) = \frac{(z^{-1} + 2 + z)^3 (3z^{-2} + 18z^{-1} + 38 + 18z + 3z^2)}{256}. \quad (3.31)$$

The corresponding analysis wavelet has six vanishing moments.

Donoho [21] presented a scheme where an odd sample is predicted by the value at the central point of a polynomial of odd degree which interpolates adjacent even samples. One can observe that our filter U_m^3 (3.30) coincides with the filter derived by Donoho's scheme using a cubic interpolatory polynomial. The filter U_e^3 (3.31) coincides with the filter derived using an interpolatory polynomial of fifth degree. Note that in Donoho's construction the *update* step does not exist. On the other hand, the filters $1+z^{-1}U_m^3(z^2)$ and $1+z^{-1}U_e^3(z^2)$ are the autocorrelations of 4-tap and 6-tap filters by Daubechies, respectively [33].

3.5.2. *Upgrade of interpolatory splines*

We can use a similar approach for increasing the approximation accuracy of interpolatory splines of odd order at midpoints. It can be done in two ways. Let S_i^{2r-1} be a spline of order $2r-1$, which interpolates a sequence $\{e_k\}$ on the grid $\{2k\}$.

Upgrade of the numerator of the transfer function: We introduce a new spline S_ρ^{2r-1} as follows: $\widetilde{S}_\rho^{2r-1} = S_i^{2r-1} + \rho S_d^{2r-1}$, $S_d^{2r-1} \stackrel{\Delta}{=} \sum_l (\mathbf{D}^{2r} e_l)\, M^{2r-1}(t/2-l)$. Then an assertion similar to Proposition 3.7 holds.

Proposition 3.8. *Let f be a polynomial of degree $2r-1$ and $e_k \stackrel{\Delta}{=} \{f(2k)\}$, $k \in \mathbb{Z}$. Then for any real ρ the spline $\widetilde{S}_\rho^{2r-1}(2k+1) \equiv f(2k+1)$, $\widetilde{S}_\rho^{2r-1}(2k) \equiv f(2k)$, $k \in \mathbb{Z}$. However, if f is a polynomial of degree $2r+1$ and $\rho = 4^{-r}A_{2r-1}$, where A_{2r-1} is defined in (3.16), then the spline restores values of f at the midpoints $\{2k+1\}$, $k \in \mathbb{Z}$.*

We denote the spline with $\rho = 4^{-r}A_{2r-1}$ by $\widetilde{S}_A^{2r-1}$. As before, we use values of the spline at midpoints as prediction of the odd subarray of the processed signal. Using (3.25) and (3.4), we get that the corresponding prediction filter is

$$\begin{aligned}\widetilde{U}_A^{2r-1}(z) &= U_i^{2r-1}(z) + 4^{-r}A_{2r-1}w^{2r-1}(z)(z-2+z^{-1})^r \\ &= \frac{w^{2r-1}(z)(1+4^{-r}A_{2r-1}\,u^{2r-1}(z)\,(z-2+z^{-1})^r)}{u^{2r-1}(z)}.\end{aligned}$$

By this means we update the numerator of the rational transfer function of the filter $U_i^{2r-1}(z)$. In other words, we change the FIR component of the filter.

Upgrade of the denominator of the transfer function: Another way consists of modifying the denominator rather than the numerator of the transfer function. As is seen from (3.5), the Laurent polynomial $u^{2r-1}(z)$ can be represented as the sum $u^{2r-1}(z) = 1 + \sum_{k=1}^{r-1}\alpha_k(z-2+z^{-1})^k$.

We introduce a new Laurent polynomial

$$u_\rho^{2r-1}(z) \triangleq 1+\sum_{k=1}^{r-1} \alpha_k (z-2+z^{-1})^k + \rho(z-2+z^{-1})^r = u^{2r-1}(z)+\rho(z-2+z^{-1})^r \tag{3.32}$$

and the rational function $\check{U}_\rho^{2r-1}(z) \triangleq w^{2r-1}(z)/u_\rho^{2r-1}(z)$. Similarly to the construction of the interpolatory splines we define the quasi-fundamental spline

$$L_\rho^{2r-1}(x) \triangleq \sum_l \lambda_{\rho,l}^{2r-1}\, M^{2r-1}(x-l), \quad \sum_{k=-\infty}^{\infty} z^{-k} \lambda_{\rho,k}^{2r-1} = \frac{1}{u_\rho^{2r-1}(z)}. \tag{3.33}$$

Given a sequence $\{e_k\}$, we construct the spline $\check{S}_\rho^{2r-1}(t) = \sum_{l=-\infty}^{\infty} e_l\, L_\rho^{2r-1}(t/2-l)$.

Proposition 3.9. *Let f be a polynomial of degree $2r-1$ and $\mathbf{f} \triangleq \{f(2k)\}$. Then for any real real ρ such that $u_\rho^{2r-1}(e^{i\omega}) \neq 0\ \forall \omega \in \mathbb{R}$, the spline $\check{S}_\rho^{2r-1}(2k+1) \equiv f(2k+1)$, $\widetilde{S}_\rho^{2r-1}(2k) \equiv f(2k)$, $k \in \mathbb{Z}$. However, if $f(t)$ is a polynomial of degree $2r+1$ and $\rho = -A_r/4^r$, where A_r is defined in (3.16), then the spline restores its values at the midpoints $\{2k+1\}$, $k \in \mathbb{Z}$.*

Proof. We can represent the difference as

$$f(2k+1) - \check{S}_\rho^{2r-1}(2k+1) = \sum_{n\in\mathbb{Z}} a^p_{\rho,2k+1-n} f(n),$$

where the z-transform of the sequence $\{a^p_{\rho,k}\}$ is $A^p_\rho(z) = 1 - z^{-1}\check{U}_\rho^{2r-1}(z^2)$. Then, using (3.15) we have

$$1 - z^{-1}\check{U}_\rho^{2r-1}(z^2) = (z-2+z^{-1})^r \frac{q(z-2+z^{-1}) + \rho(z+2+z^{-1})^r}{u^{2r-1}(z^2) + \rho(z^2-2+z^{-2})^r}$$
$$= (z-2+z^{-1})^r \frac{A_r + \rho\, 4^r + \sum_{k=1}^r \nu_k (z-2+z^{-1})^k}{u^{2r-1}(z^2) + \rho(z^2-2+z^{-2})^r}.$$

Hence, the assertion of the proposition concerning the midpoints $\{2k+1\}$ follows. As for the points $\{2k\}$, it is seen from (3.33) that the difference is $f(2k) - \check{S}_\rho^{2r-1}(2k) = \sum_n b^p_{\rho,k-n} f(2n)$, where the z-transform of the sequence $\{b^p_{\rho,k}\}$ is

$$B^p_\rho(z) = 1 - \frac{u^{2r-1}(z)}{u_\rho^{2r-1}(z)} = \frac{\rho(z-2+z^{-1})^r}{u_\rho^{2r-1}(z)}.$$

Therefore, the spline interpolates polynomials of degree $2r-1$ at the points $\{2k\}$. □

Examples:

Quadratic spline with upgraded numerator:

$$\tilde{U}_A^{2r-1}(z) = \frac{(1+z)(1024+(z^{-1}+6+z)(z^{-1}-2+z)^2)}{256(z^{-1}+6+z)}$$

$$1 - z^{-1}\tilde{U}_A^{2r-1}(z^2) = \frac{(z-2+z^{-1})^3}{256\,(z^2+6+z^{-2})} \times$$

$$\times \left(z^4 + 6\,z^3 + 24\,z^2 + 74\,z + 174 + 74\,z^{-1} + 24\,z^{-2} + 6\,z^{-3} + z^{-4}\right).$$

Quadratic spline with upgraded denominator:

$$\check{U}_A^{2r-1}(z) = \frac{64(1+z)}{16(z^{-1}+6+z) - (z^{-1}-2+z)^2}$$

$$1 - z^{-1}\check{U}_A^{2r-1}(z^2) = \frac{-(z-2+z^{-1}))^3(z+6z+1/z)}{16(z^{-2}+6+z^2) - (z^{-2}-2+z^2)^2}.$$

4. Design of prediction filters using discrete splines

In this section we derive prediction filters for lifting wavelet transforms using the so-called discrete splines. We will show that these filters are intimately related to the Butterworth filters which are commonly used in signal processing [28].

4.1. *Discrete splines*

We outline briefly the properties of discrete splines, which will be needed for further constructions. For a detailed description of the subject, see [29] [32]. The discrete splines are defined on the grid $\{k\}$ and present a counterpart to the continuous polynomial splines.

The discrete B-spline of first order is defined by the following sequence for $k \in \mathbb{Z}$:

$$B_k^{1,n} = \begin{cases} 1 \;\text{ if } k = 0, \ldots, 2n-1,\; n \in \mathbb{N}, \\ 0, \text{ otherwise.} \end{cases}$$

We define by recurrence the higher order B-splines via the discrete convolutions: $B^{p,n} = B^{1,n} * B^{p-1,n}$. Obviously, the z-transform of the B-spline of order p is

$$B^{p,n}(z) = (1 + z^{-1} + z^{-2} + \ldots + z^{-2n+1})^p \quad p = 1, 2, \ldots.$$

In this paper we are interested only in the case when $p = 2r,\ r \in \mathbb{N}$ and $n = 1$. In this case we have $B^{2r,1}(z) = (1+z^{-1})^{2r}$. The B-spline $B_k^{2r,1}$ is symmetric about the point $k = r$ where it attains its maximal value. We define the centered B-spline M_k^{2r} of order $2r$ as the shift of the B-spline:

$$M_k^{2r} \triangleq B^{2r,1}(k+r), \quad M^{2r}(z) = z^r B^{2r,1}(z) = z^r(1+z^{-1})^{2r}. \tag{4.1}$$

The discrete spline of order $2r$ is defined as a linear combination, with real-valued coefficients,

$$S_k^{2r} \triangleq \sum_{l=-\infty}^{\infty} c_l M_{k-2l}^{2r} \tag{4.2}$$

of shifts of the centered B-spline of order $2r$. Our scheme to design prediction filters using the discrete splines remains the same as the above scheme, that is based on polynomial interpolatory splines. Namely, we construct the discrete spline, which interpolates even samples $\{e_k = f_{2k}\}$ of a signal $\mathbf{f} \triangleq \{f_k\},\ k \in \mathbb{Z}$, and use the values S^{2r}_{2k+1} for the prediction of odd samples $\{o_k = f_{2k+1}\}$. As in Section 3.3 we denote by $\mathbf{s}^e \triangleq \{s_{e,k} \triangleq S^{2r}_{2k}\}$, $\mathbf{s}^o \triangleq \{s_{o,k} \triangleq S^{2r}_{2k+1}\}$ and $\mathbf{s} = \{s_k \triangleq S^{2r}_k\}$ the values of the spline at grid points, at midpoints and in the whole set $\{k\}$, respectively.

We construct the spline S^{2r}_d such that

$$S^{2r}_{2k} = s_{e,k} = e_k,\ k \in \mathbb{Z}. \tag{4.3}$$

Let $e(z)$ be the z-transform of the sequence $\{e_k\}$.

Proposition 4.1. *The $z-$transform of the sequence $\mathbf{s}^o$ of values of the discrete spline at midpoints is*

$$\begin{aligned} &s^o(z) = U^{2r}_d(z)e(z),\ U^{2r}_d(z) \triangleq \frac{\theta^{2r}(z)}{\upsilon^{2r}(z)}, \\ &\upsilon^{2r}(z^2) \triangleq \frac{1}{2}\left(z^r\left(1+z^{-1}\right)^{2r} + (-z)^r\left(1-z^{-1}\right)^{2r}\right), \\ &\theta^{2r}(z^2) \triangleq \frac{z}{2}\left(z^r\left(1+z^{-1}\right)^{2r} - (-z)^r\left(1-z^{-1}\right)^{2r}\right). \end{aligned} \tag{4.4}$$

Proof. Applying the z-transform to Eq. (4.2), we get:

$$s(z) = C(z^2)M^{2r}_e(z^2) + z^{-1}C(z^2)M^{2r}_o(z^2) = s^e(z^2) + z^{-1}s^o(z^2),$$

where $C(z)$ is the z-transform of the sequence of coefficients $\{c_l\}$ and

$$M^{2r}_e(z^2) = \sum_{k\in\mathbb{Z}} z^{-2k}M^{2r}_{2k} = \upsilon^{2r}(z^2), \quad M^{2r}_o(z^2) = \sum_{k\in\mathbb{Z}} z^{-2k}M^{2r}_{2k+1} = \theta^{2r}(z^2) \tag{4.5}$$

Equations (4.3) and (4.5) imply that

$$C(z) = e(z)/\upsilon^{2r}(z), \quad s^o(z) = C(z)\theta^{2r}(z) = e(z)\frac{\theta^{2r}(z)}{\upsilon^{2r}(z)}.$$

To make sure that $s^o(z)$ has no poles as $z = e^{i\omega}$, we substitute $z = e^{i\omega}$ into $\upsilon^{2r}(z^2)$.

$$\begin{aligned} \upsilon^{2r}(z^2) &= \frac{1}{2}\left[e^{ir\omega}(1+e^{-i\omega})^{2r} + (-1)^r e^{ir\omega}(1-e^{-i\omega})^{2r}\right] \\ &= \frac{1}{2}\left[\left(2\cos\frac{\omega}{2}\right)^{2r} + \left(2\sin\frac{\omega}{2}\right)^{2r}\right] > 0. \end{aligned}$$

□

Thus the filters $U^{2r}_d(z)$ can be used as the prediction filters in the lifting scheme. They are closely related to the so-called discrete-time Butterworth filters.

4.2. *Discrete-time Butterworth filters*

We recall briefly the notion of Butterworth filter. For details we refer to [28]. The magnitude squared frequency responses $\widehat{F}_l^r(\omega)$ and $\widehat{F}_h^r(\omega)$ of the low- and high-pass digital Butterworth filters of order r, respectively, are given by the formulas

$$|\widehat{F}_l^r(\omega)|^2 = \frac{1}{1+(\tan\frac{\omega}{2}/\tan\frac{\omega_c}{2})^{2r}}, \quad |\widehat{F}_h^r(\omega)|^2 = 1-|\widehat{F}_l^r(\omega)|^2 = \frac{1}{1+(\tan\frac{\omega_c}{2}/\tan\frac{\omega}{2})^{2r}}$$

where ω_c is the so-called cutoff frequency.

We are interested in the half-band Butterworth filters, that is $\omega_c = \pi/2$. In this case

$$|\widehat{F}_l^r(\omega)|^2 = \frac{1}{1+(\tan\frac{\omega}{2})^{2r}}, \quad |\widehat{F}_h^r(\omega)|^2 = 1-|\widehat{F}_l^r(\omega)|^2 = \frac{1}{1+(\cot\frac{\omega}{2})^{2r}}.$$

If $z = e^{i\omega}$ then we obtain that the magnitude squared transfer function of the low-pass filter is:

$$|F_l^r(z)|^2 = \left(1+\frac{(-1)^r\left(1-z^{-1}\right)^{2r}}{\left(1+z^{-1}\right)^{2r}}\right)^{-1} = \frac{\left(1+z^{-1}\right)^{2r}}{\left(1+z^{-1}\right)^{2r}+(-1)^r\left(1-z^{-1}\right)^{2r}}.$$

Similarly, the magnitude squared transfer function of the high-pass filter is:

$$|F_h^r(z)|^2 = \frac{(-1)^r\left(1-z^{-1}\right)^{2r}}{\left(1+z^{-1}\right)^{2r}+(-1)^r\left(1-z^{-1}\right)^{2r}}.$$

It is readily seen that the function U_d^{2r}, defined in (4.4), is related to these transfer functions:

$$\frac{1}{2}\left(1+z^{-1}U_d^{2r}(z^2)\right) = |F_l^r(z)|^2, \quad \frac{1}{2}\left(1-z^{-1}U_d^{2r}(z^2)\right) = |F_h^r(z)|^2. \tag{4.6}$$

We will show that the structure of the filters U_d^{2r} is similar to the structure of the filters U_i^{2r-1} derived from polynomial interpolatory splines. For this purpose we analyze the denominator of the rational function $U_d^{2r}(z)$.

Proposition 4.2 ([6 25]). *If $r = 2p+1$ then:*

$$\upsilon^{2r}(z) = 2r\prod_{k=1}^{p}\frac{1}{\gamma_k^r}(1+\gamma_k^r z^{-1})(1+\gamma_k^r z), \quad \gamma_k^r = \cot^2\frac{(p+k)\pi}{2r} < 1, \quad k = 1,\ldots,p.$$

If $r = 2p$ then

$$\upsilon^{2r}(z) = \prod_{k=1}^{p}\frac{1}{\gamma_k^r}(1+\gamma_k^r z^{-1})(1+\gamma_k^r z), \quad \gamma_k^r = \cot^2\frac{(2p+2k-1)\pi}{4r} < 1,\ k = 1,\ldots,p.$$

Examples:

The simplest case, $r = 1$**:** We have

$$U_d^2(z) = \frac{1+z}{2},\ 1 + z^{-1}U_d^2(z^2) = \frac{z^{-1}+2+z}{2}. \tag{4.7}$$

The filter U_d^2 is FIR. ¿From Proposition 2.3, the high-frequency analysis wavelet $\tilde{\psi}^1$ has two vanishing moments.

Cubic discrete spline, $r = 2$**:**

$$U_d^4(z) = 4\frac{1+z}{z+6+z^{-1}}, \quad 1 + z^{-1}U_i^3(z^2) = \frac{(z+2+z^{-1})^2}{z^{-2}+6+z^2}. \tag{4.8}$$

It is readily seen that the filter U_d^4 coincides with the filter U_i^3 derived from the quadratic polynomial spline (see (3.12). The high-frequency analysis wavelet $\tilde{\psi}^1$ has four vanishing moments.

Discrete spline of sixth order, $r = 3$**:** We have

$$U_d^6(z) = \frac{(z+14+z^{-1})(1+z)}{6z^{-1}+20+6z} \quad 1 + z^{-1}U_d^6(z^2) = \frac{(z^{-1}+2+z)^3}{6z^2+20+6z^{-2}}. \tag{4.9}$$

The high-frequency analysis wavelet $\tilde{\psi}^1$ has six vanishing moments.

Discrete spline of eighth order, $r = 4$**:**

$$\begin{aligned} U_d^8(z) &= \frac{8(1+z)(z^{-1}+6+z)}{z^{-2}+28z^{-1}+70+28z+z^2}, \\ 1 + \frac{U_d^8(z^2)}{z} &= \frac{(z^{-1}+2+z)^4}{z^{-4}+28z^{-2}+70+28z^2+z^4}. \end{aligned} \tag{4.10}$$

The high-frequency analysis wavelet $\tilde{\psi}^1$ has eight vanishing moments.

5. Filters for the *update* step

In Sections 3 and 4 we presented a family of filters U for the *predict* step, which was derived from splines of various types. To complete the construction of the transform we need to define the filter V for the *update* part. The fact that any choice of these filters retains the perfect reconstruction property of the transform is a great advantage of the lifting scheme. Proposition 2.3 indicates that, in order to produce synthesis and analysis filters with similar properties, it is advisable to choose $V(z) = \breve{U}(1/z)$, where $\breve{U}$ is one of the filters U presented above. In particular, the filter $\breve{U}$ may coincide with the filter U, which is used for the prediction. In this case the numbers of vanishing moments of the high-frequency analysis and synthesis wavelets are equal to each other. On the other hand, by combining various pairs of the prediction U and the update $V(z) = \breve{U}(1/z)$ filters, we obtain a wide family of biorthogonal wavelet s with diverse properties. Implementation of derived filters with rational transfer functions is discussed in details in [10].

6. Scaling functions and wavelets generated by rational filters

Cascade algorithm and subdivision schemes We presented in previous sections a set of filters U and V, which are used as prediction and update filters in lifting schemes. They produce a family of perfect reconstruction filter banks H, G, $\widetilde{H}$ and $\widetilde{G}$ (see Section 2.2). These filter banks generate analysis and synthesis scaling functions $\widetilde{\varphi}$, which are solutions for the refinement equations [16]:

$$\widetilde{\varphi}(t) = \sqrt{2}\sum_{k\in\mathbb{Z}} \tilde{h}_k \widetilde{\varphi}(2t-k), \quad \varphi(t) = \sqrt{2}\sum_{k\in\mathbb{Z}} h_k \varphi(2t-k). \tag{6.1}$$

The cascade algorithm for the construction of scaling functions, which is described in [16], consists of infinite iterations of the subdivision scheme whose mask is either the low-pass synthesis filter A, or the analysis filter $\widetilde{A}$, whose symbols are

$$a(z) = \sqrt{2}H(z) = 1 + z^{-1}U(z^2), \quad \tilde{a}(z) = \sqrt{2}\tilde{H}(z) = 2 + zV(z^2) - V(z^2)U(z^2), \tag{6.2}$$

respectively. This scheme is applied to the initial data, which is the Kroneker delta δ_n. If this process converges then the limit function, which is called the basic limit function (BLF) of the subdivision scheme, is the scaling function generated by either the filter H or $\widetilde{H}$ ([16]). Therefore, methods of analysis of convergence and of regularity of limit functions, which have been developed in the theory of subdivision schemes, can be applied to the analysis of scaling functions. Our analysis is based on a technique developed in [22 23] for the schemes that employ FIR filters. The extension of the technique to schemes with IIR filters requires some modifications. We outline briefly our results on the convergence of the subdivision schemes with rational symbols and the properties of the corresponding scaling functions and wavelets. A detailed presentation of these results is given in [49].

A univariate stationary uniform subdivision scheme S_a that is based on a filter $a(z) = \sum_{k\in\mathbb{Z}} z^{-k}a_k$, consists of the following:

Given the initial data $\mathbf{f^0} = \{f_k^0\}$, $k \in \mathbb{Z}$, one refinement step is an extension of the function f^j, $j = 0, 1, \ldots$, defined on the grid $\mathbf{G^j} = \{k/2^j\}_{k\in\mathbb{Z}}$: $f^j(k/2^j) = f_k^j$, onto the grid $\mathbf{G^{j+1}}$ by multirate filtering the array $\{f_k^j\}$:

$$f_k^{j+1} = \sum_{l\in\mathbb{Z}} a_{k-2l} f_l^j. \tag{6.3}$$

The insertion rule (6.3) splits into two separate rules: $f_{2k}^{j+1} = \sum_{l\in\mathbb{Z}} a_{k-l}^e f_l^j$, $f_{2k+1}^{j+1} = \sum_{l\in\mathbb{Z}} a_{k-l}^o f_l^j$, where $a_k^e \triangleq a_{2k}$ and $a_k^o \triangleq a_{2k+1}$. The impulse response $\mathbf{a} = \{a_k\}$ of the filter $a(z)$ is called the refinement mask of the subdivision scheme S_a. If $a_0 = 1$, $a_{2k} = 0\ \forall k \neq 0$ then the subdivision scheme is interpolatory (ISS). In this case $f_{2k}^{j+1} = f_k^j$. The transfer function $a(z)$ of the filter is called the symbol of the subdivision scheme S_a. Provided f^j and f^{j+1} belong to the space l^1, Eq. (6.3) is equivalent to the following relation in the z-domain:

$$f^{j+1}(z) = a(z)f^j(z^2). \tag{6.4}$$

Comparing (6.4) with (2.4), we see that this refinement step is completely identical to the reconstruction of the signal $\mathbf{x}$ from the array $\mathbf{s^1}$, provided $a(z) = H(z)$. It is apparent that all the synthesis filters presented in Sections 3 and 4 are associated with the interpolatory subdivision schemes.

Definition 6.1. *Let the initial data be* $\mathbf{f^0} = \{f_k^0\},\ k \in \mathbb{Z}$ *and* $\{f^j(t)\},\ j \in \mathbb{N}$, *be the sequence of continuous functions that interpolate the data generated by* S_a *at the corresponding refinement level:* $\{f^j(2^{-j}k) = f_k^j = (S_a^j f^0)_k\},\ k \in \mathbb{Z}$. *If* $\{f^j(t)\}$ *converges uniformly at any finite interval to a continuous function* $f^\infty(t)$ *as* $j \to \infty$ *then we say that the subdivision scheme* S_a *converges on the initial data* $\mathbf{f^0}$ *and* $f^\infty(t)$ *is called its limit function.*

Definition 6.2. *If the scheme converges on the initial data* $\{f_k^0 = \delta_k\},\ k \in \mathbb{Z}$, *(Kroneker delta), then the limit function, which we denote as* ϕ_a, *is called the basic limit function (BLF) of the scheme* S.

Proposition 6.1 ([16]). *The BLF of the scheme* S_a *is the scaling function of the wavelet transform whose low-pass filter is* $a(z)$.

All the above designed filters generate subdivision schemes S_a, whose symbols $a(z) = V(z)/P(z)$ are rational functions and possess the following properties:

P1: The Laurent polynomials $P(z)$ and $V(z)$ are invariant under the inversion $P(z^{-1}) = P(z)$, $V(z^{-1}) = V(z)$ and thus are real on the unit circle $|z| = 1$.

P2: Roots of the denominator $P(z)$ are real, simple and do not lie on the unit circle $|z| = 1$.

P3: $P(z)$ can be represented as follows:

$$P(z) = \prod_{n=1}^{r} \frac{1}{\gamma_n}(1+\gamma_n z)(1+\gamma_n z^{-1}), \quad 0 < |\gamma_1| < \ldots |\gamma_r| = e^{-g} < 1,\ g > 0, \tag{6.5}$$

and, for all k $\operatorname{Im}\gamma_k = 0$. If **P1** and **P2** hold then they imply **P3**.

P4: The symbol $a(z)$ can be factorized as follows:

$$a(z) = (1+z)q(z), \quad q(1) = 1. \tag{6.6}$$

Definition 6.3. *We say that a rational function* $a(z)$ *belongs to Class* $\boldsymbol{P}$ *if it possesses all the properties* ***P1****–* ***P4****.*

The above properties imply in particular that the coefficients a_k of the mask of a Class **P** scheme S_a are symmetric about zero.

Proposition 6.2 ([49]). *If the symbol of a scheme* S_a *is* $a(z) = V(z)/P(z)$ *and Eq. (6.5) holds then the mask*

$$|a_k| \le A\, e^{-g|k|},$$

where A *is a positive constant.*

Denote $\|\mathbf{f^j}\|_\infty \stackrel{\Delta}{=} \max_{k\in\mathbb{Z}} |f_k^j|$. Eq. (6.3) implies that $f_{2k}^{j+1} = \sum_{l\in\mathbb{Z}} a_{2k-2l} f_l^j$, $f_{2k+1}^{j+1} = \sum_{l\in\mathbb{Z}} a_{2k+1-2l} f_l^j$. Hence, it follows that $\|\mathbf{f^{j+1}}\|_\infty \le \|S_a\| \, \|\mathbf{f^j}\|_\infty$, where $\|S_a\| \stackrel{\Delta}{=} \max\left\{\sum_{k\in\mathbb{Z}} |a_{2k}|, \ \sum_{k\in\mathbb{Z}} |a_{2k+1}|\right\}$. Similarly, after L refinement steps we have $\|\mathbf{f^{j+L}}\|_\infty \le \|S_a^L\| \, \|\mathbf{f^j}\|_\infty$, where

$$\|S_a^L\| \stackrel{\Delta}{=} \max_i \left\{ \sum_k |a_{i+2^L k}^{[L]}| : 0 \le i \le 2^L - 1 \right\}$$

and $\left\{a_k^{[L]}\right\}$ is the mask of the operator S_a^L.

Definition 6.4. *If for some $L \in \mathbb{N}$ the following inequality holds*

$$\|S_a^L\| \stackrel{\Delta}{=} \max_i \left\{ \sum_k |a_{i+2^L k}^{[L]}| : 0 \le i \le 2^L - 1 \right\} = \mu < 1 \tag{6.7}$$

then the scheme S_a is called contractive.

Convergence of the cascade algorithm and regularity of scaling functions Let S_a be a subdivision scheme, whose mask $\mathbf{a} = \{a_k, \ k \in \mathbb{Z}\}$ and symbol is $a(z)$. To establish the existence of the continuous scaling function associated with the filter $a(z)$, it is sufficient to prove the convergence of the subdivision scheme S_a on the initial data $\mathbf{f^0} = \{\delta_k, \ k \in \mathbb{Z}\}$. However, a more general proposition is proved in [49].

Proposition 6.3 ([49]). *Let S_a be a subdivision scheme of Class $\boldsymbol{P}$, whose symbol is $a(z) = (1+z)q(z)$, and S_q be the scheme, whose symbol is $q(z)$ and mask is $\{q_k\}$, $k \in \mathbb{Z}$. If the scheme S_q is contractive then the scheme S_a converges on any initial data $\mathbf{f^0} \in l^1$.*

The smoothness of the scaling functions is determined by the following proposition.

Proposition 6.4 ([22]). *Let S_a be a subdivision scheme of Class $\boldsymbol{P}$ and in addition let the symbol be factorized as follows: $a(z) = 2^{-m}(1+z)^m b(z)$. If for some initial data $\mathbf{f^0} \in l_1$ the subdivision scheme S_b, whose symbol is $b(z)$, converges on the data $\mathbf{g^0} \stackrel{\Delta}{=} \mathbf{\Delta^m f^0}$ to a continuous function $g^\infty(t)$ then the scheme S_a converges on the data f^0 to a function $f^\infty(t)$, $t \in \mathbb{R}$, which has m continuous derivatives and $f^\infty(t)^{(m)} = g^\infty(t)$.*

Exponential decay of BLF's We proved in [49] that the basic limit function of a convergent subdivision scheme with the rational symbol decays exponentially as its argument tends to infinity. Hence it follows the result concerned with the scaling functions.

Theorem 6.1. *Let a low-pass filter $H(z) = a(z)/\sqrt{2}$ and $a(z)$ be a function of Class $\boldsymbol{P}$. If the subdivision scheme S_q, whose symbol is $q(z) = a(z)/(1+z)$, is contractive*

then the filter $H(z)$ generates a continuous scaling function $\varphi_H(t)$, which decays exponentially as $|t| \to \infty$. Namely, if (6.5) holds then for any $\varepsilon > 0$ there exists a constant $\Phi_\varepsilon > 0$ such that the following inequality is true: $|\varphi_H(t)| \le \Phi_\varepsilon\, e^{-(g-\varepsilon)t}$.

Let the filter $a(z)$ satisfy the conditions of Theorem 6.1 and in addition be factorized as follows: $a(z) = 2^{-m}(1+z)^{m+1}q^{[m]}(z)$, where $q^{[m]}(1) = 1$. If the subdivision scheme $S_q^{[m]}$, whose symbol is $q^{[m]}(z)$, is contractive then the scaling function $\varphi_H(t)$ has m continuous derivatives.

The analysis and synthesis scaling functions $\widetilde{\varphi}$ and φ, which satisfy the refinement equations (6.1) generate the analysis and synthesis wavelets $\widetilde{\psi}$ and ψ, respectively, via the two-scale equations

$$\widetilde{\psi}(t) = \sqrt{2}\sum_{k\in\mathbb{Z}} \widetilde{g}_k \widetilde{\varphi}(2t-k), \quad \psi(t) = \sqrt{2}\sum_{k\in\mathbb{Z}} g_k \varphi(2t-k), \tag{6.8}$$

where $\{\widetilde{g}_k\}$ and $\{g_k\}$ are the impulse responses of the high-pass filters $\tilde{G}$ and G, respectively. Equations (2.2) imply the rational functions $\tilde{G}(z)$ and $G(z)$ have no poles on the unit circle and, therefore, the sequences $\{\widetilde{g}_k\}$ and $\{g_k\}$ decay exponentially. Then it follows from (6.8) that the wavelets $\widetilde{\psi}(t)$ and $\psi(t)$ decay exponentially as $t \to \infty$. Moreover, the smoothness of the wavelets $\widetilde{\psi}$ and ψ is the same as the smoothness of the scaling functions $\widetilde{\varphi}$ and φ, respectively.

Definition 6.5. *A wavelet ψ has n vanishing moments if the following relations hold*

$$\int_{-\infty}^{\infty} t^k \psi(t)\, dt = 0, \quad k = 0, \dots n-1.$$

Proposition 6.5 ([34]). *If the low-pass synthesis filter $H(z)$ has n zeros at $z = -1$ then the analysis wavelet $\widetilde{\psi}$ has n vanishing moments. If the low-pass analysis filter $\widetilde{H}(z)$ has $\tilde{n}$ zeros at $z = -1$ then the synthesis wavelet ψ has $\tilde{n}$ vanishing moments.*

In our scheme this fact can be reformulated in a form similar to Proposition 2.3

Proposition 6.6. *Let the functions $U(z)$ and $V(z)$, which are used for the* predict *and* update *steps, respectively, be rational and have no poles on the unit circle $|z| = 1$. Let $1+z^{-1}U(z^2)$ comprise the factor $(z+2+z^{-1})^r$ and $1+zV(z^2)$ comprise the factor $(z+2+z^{-1})^p$. If the analysis and synthesis scaling functions exist then the analysis wavelet $\tilde{\psi}$ has $2r$ vanishing moments and the synthesis wavelet ψ has $2s$ vanishing moments, where $s = \min(p, r)$.*

Scaling functions generated by polynomial splines of even order In the case when the prediction filter is derived from a polynomial interpolatory spline of even order, as was described in Section 3.3, the synthesis scaling function and wavelet are splines of the same order.

Theorem 6.2.

1. *If the prediction filter in the lifting scheme $U_i^{2r}(z)$ is derived from a polynomial interpolatory spline of order $2r$ then the cascade algorithm for the construction of the synthesis scaling function $\varphi(t)$ converges for any r and $\varphi(t) = L^{2r}(t)$, where $L^{2r}(t)$ is the fundamental spline of order $2r$ with nodes on the grid $\{k\}_{k\in\mathbb{Z}}$. This spline was defined in (3.23).*

2. *If, in addition, the update filter $V(z)$ is chosen as suggested in Section 5 then the synthesis wavelet $\psi(t)$ is the spline $\sigma^{2r}(t)$, which interpolates the data $\sqrt{2}\{g_k\}$, where $\{g_k\}$ is the impulse response of the synthesis high-pass filter $G(z) \triangleq \sqrt{2}z^{-1}\left(1 - zV(z^2)\left(1 + z^{-1}U_i^{2r}(z^2)\right)/2\right)$ on the grid $\{k/2\}$, $k \in \mathbb{Z}$.*

Proof.

1. We consider a subdivision scheme S_a with the symbol $a(z) = 1 + z^{-1}U_i^{2r}(z^2)$ derived from an interpolatory spline of degree $2r$. Let the initial data be $\mathbf{f^0} = \{\delta_k\}$ and $\{f^j(t)\}$, $j = 0, 1, \ldots$ be a sequence of splines of order $2r$ constructed on the grid $\{2^{-j}k\}$ that ıe the subsequently refined data at grid points, that is, $f^j(2^{-j}k) = f_k^j$, $k \in \mathbb{Z}$. We show by induction that for all non-negative integers j the splines $f^j(t) = L^{2r}(t)$. Obviously, it is true for $f^0(t)$. Suppose that for some $j \in \mathbb{N}$ we have $f^{j-1}(t) = L^{2r}(t)$. Due to the well known property of minimal norm [2], the integral

$$\mu \triangleq \int_{-\infty}^{\infty} |(L^{2r})^{(r)}(t)|^2\, dt \le \int_{-\infty}^{\infty} |q^{(r)}(t)|^2\, dt,$$

where $q(t)$ is any function such that $q^{(r)}(t)$ is square summable and $q(k) = \delta_k$. The refined data is $f_k^j = f^{j-1}(2^{-j}k) = L^{2r}(2^{-j}k)$. For the spline $f^j(t)$, which interpolates this data, we have the inequality

$$\nu \triangleq \int_{-\infty}^{\infty} |(f^j)^{(r)}(t)|^2\, dt \le \int_{-\infty}^{\infty} |Q^{(r)}(t)|^2\, dt,$$

where $Q(t)$ is any function such that $Q^{(r)}(t)$ is square summable and $Q(2^{-j}k) = L^{2r}(2^{-j}k)$. Hence, $\nu \le \mu$. On the other hand, $f_k^j = \delta_k$ and, therefore, $\mu \le \nu$. Thus,

$$\int_{-\infty}^{\infty} |(L^{2r})^{(r)}(t)|^2\, dt = \int_{-\infty}^{\infty} |(f^j)^{(r)}(t)|^2\, dt.$$

Hence, it follows that $f^j(t) \equiv L^{2r}(t)$. Thus the first claim of the theorem is proved.

2. Under conditions of the theorem the synthesis wavelet $\psi(t)$ is derived from the scaling function $\varphi(t) = L^{2r}(t)$ via the two-scale equation

$$\psi(t) = \sqrt{2}\sum_{k\in\mathbb{Z}} g_k L^{2r}(2t - k), \tag{6.9}$$

where $\{g_k\}$ is the impulse response of the high-pass filter G. But the series in (6.9) represents a spline of order $2r$, which interpolates $\sqrt{2}\{g_k\}$ on the grid $\{k/2\}$, $k \in \mathbb{Z}$. □

Remark. Note that the analysis scaling function and wavelet are not splines. Also for the schemes that use splines of odd order, the synthesis as well as the analysis scaling functions and wavelets are not splines. However, due to the superconvergence property, in this case the synthesis scaling function and wavelet are smoother then the generating splines.

Evaluation of the coefficients of the subdivision mask The above propositions yield a practical algorithm that establishes the convergence of a subdivision scheme and analyzes its regularity. The key operation is the evaluation of sums of type (6.7) of the mask coefficients when the symbol $a(z) = \sum_{k\in\mathbb{Z}} z^{-k} a_k$ is available. For subdivision schemes with finite masks these sums can be calculated directly. But for infinite masks different methods of evaluation of the coefficients are required. We outline a method based on the discrete Fourier transform (DFT) . More details are given in [49].

We consider the case when the number L in Eq. (6.7) is 1. The cases $L > 1$ are similarly treated. Thus, we need to evaluate the sums $\sigma_e(a) = \sum_{k=-\infty}^{\infty} |a_{2k}|, \quad \sigma_o(a) = \sum_{k=-\infty}^{\infty} |a_{2k+1}|$. We assume that $N = 2^p$, $p \in \mathbb{N}$. We denote $A(\omega) = a(e^{i\omega} = \sum_{k=-\infty}^{\infty} e^{-i\omega k}\, a_k$. and calculate this function in the discrete set of points:

$$\widehat{a}_n = A\left(\frac{2\pi n}{N}\right) = \sum_{k=-\infty}^{\infty} e^{\frac{-2\pi i k n}{N}}\, a_k = \sum_{r=-N/2}^{N/2-1} e^{\frac{-2\pi i r n}{N}}\, \theta_r, \quad \theta_r \triangleq \sum_{l=-\infty}^{\infty} a_{r+lN}.$$

The samples θ_k are available via the inverse DFT:

$$\theta_r = \frac{1}{N} \sum_{r=-N/2}^{N/2-1} e^{\frac{2\pi i r n}{N}} \widehat{a}_n.$$

Thus the sums we are interested in are evaluated as follows:

$$\sigma_e(a) = \sum_{r=-N/4}^{N/4-1} |\theta_{2k}| + \rho_N, \quad \rho_N \le B(N+2)\gamma^N,$$

where $B > 0$ $\gamma \in (0,1)$ and some constants. Hence, it follows that by doubling N, we can approximate the infinite series $\sigma_e(a)$ by the finite sum $\sigma_e^N(a) = \sum_{r=-N/4}^{N/4-1} |\theta_{2k}|$, whose terms are available via the DFT. Practically, we can iterate calculations by gradually doubling N until the result of calculating $\sigma_e^{2N}(a)$ becomes identical to $\sigma_e^N(a)$ (up to machine precision). The same approach is valid for evaluating the sum $\sigma_o(a)$ and the sums $\sum_k |q^{[L]}_{i-2^L k}|$ for any L.

7. Examples

Different combinations of the prediction and update filters, which were designed in Sections 3 and 4 enable to design a practically infinite variety of biorthogonal

wavelet transforms with symmetric waveforms. Some of them proved to be efficient in our image compression experiments. The results of these experiments are presented in [10]. In this section we summarize properties of a few such transforms and provide graphical illustration.

7.1. *List of filters*

We describe transforms, which use the following six filters:

Not.	Fil.	Source	Eq.	I.R.
F_1	U_i^3	quadratic interpolatory spline	(3.12)	IIR
F_2	U_m^3	quadratic minimal quasi-interpolatory spline	(3.30)	FIR
F_3	U_d^6	interpolatory discrete spline of sixth degree	(4.9)	IIR
F_4	U_e^3	quadratic extended quasi-interpolatory spline	(3.31)	FIR
F_5	U_d^8	interpolatory discrete spline of eighth degree	(4.10)	IIR
F_6	U_m^3	interpolatory polynomial spline of fourth degree	(3.14)	IIR

Remark: We recall that the synthesis scaling function generated by the FIR filters $F^2(z)$ and $F_4(z)$ are the autocorrelations of the scaling functions generated by the 4-tap and 6-tap Daubechies filters, respectively (see [33]).

By combining the above six filters we construct a number of transforms, which we label as $\mathbf{P}_p\mathbf{U}_u$. Here p means the index of the filter F_k, which is used for the *predict* step in the lifting scheme and u is the index of the filter, which is used for the *update* step. For example, $\mathbf{P}_1\mathbf{U}_3$ designates the transform, which performs the *predict* step using the filter $F^1(z)$ and the *update* step using the filter $F_3(z)/z$.

Proposition 7.1. *The synthesis $\varphi(x)$ and the analysis $\widetilde{\varphi}(x)$ scaling functions associated with the transforms $\boldsymbol{P}_p\boldsymbol{U}_u$ are continuous and, if the filters F_u and F_p are FIR then $\varphi(x)$ and $\widetilde{\varphi}(x)$ have compact support; if F_u is IIR and F_p is FIR then $\widetilde{\varphi}(x)$ decays exponentially as $|x| \to \infty$ and $\varphi(x)$ has compact support; if F_p is IIR then $\varphi(x)$ and $\widetilde{\varphi}(x)$ decay exponentially as $|x| \to \infty$.*

7.2. *Summary of properties of the wavelet transforms*

We summarize in Table 1 the properties of the transforms, which we employed in our image compression experiments [10]. In those experiments we compare the results produced by our transforms with the results achieved by application of the popular 9/7 biorthogonal transform ([4]), which we denote by **B**9/7. Therefore, we add to the table the properties of **B**9/7.

The following abbreviations are used in the table:

VmA: Number of vanishing moments of the analysis wavelet $\widetilde{\psi}$. **VmS**: Number of vanishing moments of the synthesis wavelet ψ. **RegA**: Regularity of the analysis scaling function $\widetilde{\varphi}$. C^k means that $\widetilde{\varphi}$ is continuous together with its k derivatives. **RegS**: Regularity of the synthesis scaling function φ. **Add**: Number of additions per pixel in the implementation of one step of the two-dimensional transforms. **Mult**:

The same for multiplications. **LFA**: Length of the analysis filter $\widetilde{H}$. **LFS**: Length of the synthesis filter H.

Transform	VmA	VmS	RegA	RegS	Add	Mult	LFA	LFS
$\mathbf{P}_1\mathbf{U}_1$	4	4	C^1	C^2	8	6	∞	∞
$\mathbf{P}_2\mathbf{U}_2$	4	4	C^0	C^1	8	4	11	5
$\mathbf{P}_3\mathbf{U}_3$	6	6	C^2	C^4	12	6	∞	∞
$\mathbf{P}_4\mathbf{U}_4$	6	6	C^1	C^2	12	6	15	7
$\mathbf{P}_1\mathbf{U}_3$	4	6	C^1	C^4	10	7	∞	∞
$\mathbf{P}_2\mathbf{U}_4$	4	6	C^0	C^2	10	5	13	5
$\mathbf{P}_5\mathbf{U}_5$	8	8	C^4	C^5	16	12	∞	∞
$\mathbf{P}_6\mathbf{U}_6$	6	6	C^2	C^4	16	12	∞	∞
$\mathbf{B}7/9$	4	4	C^0	C^1	8	4	9	7

Table 1. Properties of the transforms employed in the image compression experiments.

Comments on Table 1.

- The computational complexity is calculated under the assumption that all the presented $\widehat{s}$ are carried out through lifting steps and filtering with IIR filters is implemented in cascade mode with special treatment of the boundaries of the images [10] [28].
- Factorization of the $\mathbf{B}9/7$ transform , as suggested in [5] [18], speeds up the computation. The number of operations in Table 1 is calculated with respect to this factorization algorithm.
- It is clear from the table that the cost of the implementation of the transforms $\mathbf{P}_1\mathbf{U}_1$, $\mathbf{P}_3\mathbf{U}_3$ and $\mathbf{P}_1\mathbf{U}_3$ is close to the cost of the implementation of the transform $\mathbf{B}9/7$.

7.3. *Graphical illustrations*

In the next five figures we display several filters, scaling functions and wavelets associated with the presented transforms. All the figures are identically organized. Each of them contains four pictures. If these pictures are counted from left to right then the first column displays the frequency responses of the low-pass H and the high-pass G synthesis filters, the second column displays the frequency responses of the low-pass $\widetilde{H}$ and the high-pass $\widetilde{G}$ analysis filters, the third column displays the synthesis scaling function φ and the wavelet ψ, and the fourth column displays the analysis scaling function $\widetilde{\varphi}$ and the wavelet $\widetilde{\psi}$.

Comments on Figures 1–5: We observe that all the devised low-pass synthesis filters and high-pass analysis filters have flat frequency responses. It is especially

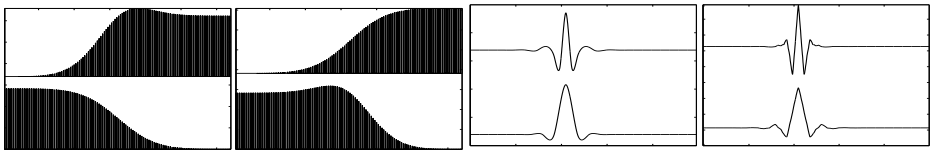

Fig. 1. Filters and wavelets associated with the $\mathbf{P}_1\mathbf{U}_1$ transform.

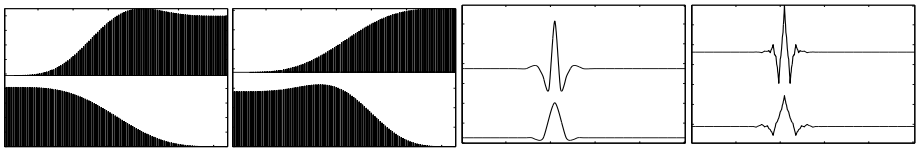

Fig. 2. Filters and wavelets associated with the $\mathbf{P}_2\mathbf{U}_2$ transform.

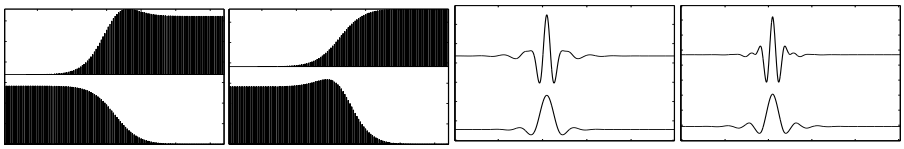

Fig. 3. Filters and wavelets associated with the $\mathbf{P}_3\mathbf{U}_3$ transform.

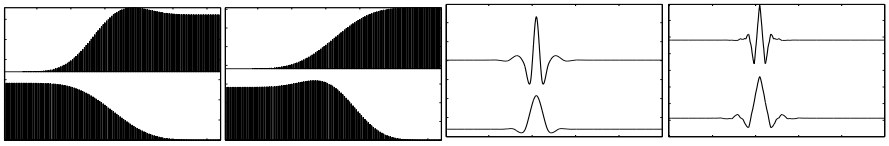

Fig. 4. Filters and wavelets associated with the $\mathbf{P}_4\mathbf{U}_4$ transform.

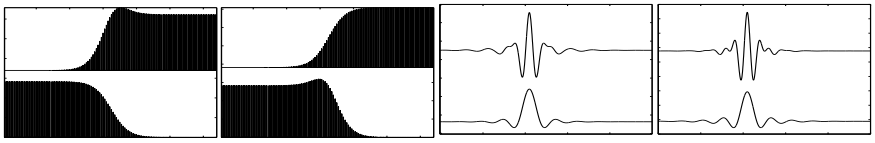

Fig. 5. Filters and wavelets associated with the $\mathbf{P}_5\mathbf{U}_5$ transform.

apparent for the IIR filters. The rest of the filters are flat up to a small bump near the cut-off. The filters of the transform $\mathbf{P}_5\mathbf{U}_5$ have the flattest frequency response and the steepest cut-off. Its scaling functions are most regular among the presented transforms.

In Figures 6 and 7 we present the derivatives of several scaling functions. Figure 6 displays second derivatives of the synthesis scaling functions of two transforms $\mathbf{P}_2\mathbf{U}_2$ and $\mathbf{P}_4\mathbf{U}_4$, which use FIR filters, and the transform $\mathbf{P}_1\mathbf{U}_1$, which uses IIR filters. Like $\mathbf{P}_2\mathbf{U}_2$, the transform $\mathbf{P}_1\mathbf{U}_1$ operates with wavelets, which have four vanishing moments. The wavelets of the $\mathbf{P}_4\mathbf{U}_4$ transform have four vanishing moments. Note that the synthesis scaling functions of $\mathbf{P}_2\mathbf{U}_2$ and $\mathbf{P}_4\mathbf{U}_4$ are the basic limit functions of the well-known 4-point and 6-point Dubuc and Deslauriers interpolatory subdivision schemes [19 20].

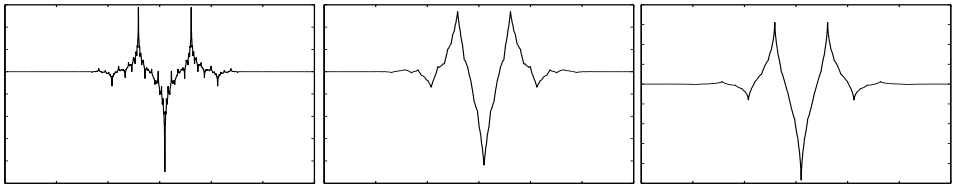

Fig. 6. Second derivatives of the synthesis scaling functions: left: $\mathbf{P}_2\mathbf{U}_2$, center: $\mathbf{P}_4\mathbf{U}_4$, right: $\mathbf{P}_1\mathbf{U}_1$.

The second derivative of the synthesis scaling function of the $\mathbf{P}_2\mathbf{U}_2$ transform does not exist. The synthesis scaling function of the $\mathbf{P}_4\mathbf{U}_4$ transform belongs to $C^\alpha,\ \alpha < 2.830$ [16 19 20]. In Figure 6 the second derivative of the synthesis scaling function of the $\mathbf{P}_1\mathbf{U}_1$ transform looks smoother than the scaling function of $\mathbf{P}_4\mathbf{U}_4$. Thus, we conjecture that the scaling function of $\mathbf{P}_1\mathbf{U}_1$ belongs to $C^\beta,\ \beta > \alpha$.

In Figure 7 we display the fourth derivatives of the synthesis scaling functions of two transforms $\mathbf{P}_3\mathbf{U}_3$ and $\mathbf{P}_6\mathbf{U}_6$, which use IIR filters. We recall that $\mathbf{P}_3\mathbf{U}_3$ is based on discrete splines of sixth order and $\mathbf{P}_6\mathbf{U}_6$ is based on polynomial splines of fifth order. Corresponding wavelets have six vanishing moments.

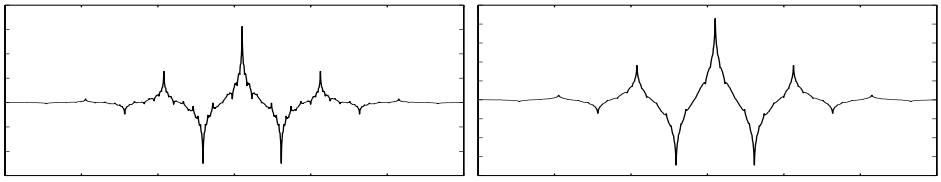

Fig. 7. Fourth derivatives of the synthesis scaling functions: left: $\mathbf{P}_3\mathbf{U}_3$, right: $\mathbf{P}_6\mathbf{U}_6$.

We observe that the fourth derivative of the scaling function of $\mathbf{P}_3\mathbf{U}_3$ has a near-fractal appearance. Nevertheless, we proved that it is continuous. Both transforms $\mathbf{P}_3\mathbf{U}_3$ and $\mathbf{P}_6\mathbf{U}_6$ have very similar properties. Also, their performance is very similar. But the computational cost to implement the $\mathbf{P}_6\mathbf{U}_6$ transform is much higher than to implement $\mathbf{P}_3\mathbf{U}_3$, and is equal to that of implementing the $\mathbf{P}_5\mathbf{U}_5$ transform, which has smoother scaling functions and wavelets with more vanishing moments.

Conclusion

In this paper we proposed an efficient technique that generates a wide range of new biorthogonal symmetric wavelet transforms. This technique is based on using discrete and polynomial interpolatory and quasi-interpolatory splines for the design of filters for the *predict* and *update* operations in lifting schemes of the wavelet transform. These are the linear phase filters which have flat frequency response. By combining different designed filters for the *predict* and *update* steps, we can devise practically unlimited types of wavelets that are as smooth as required and have a predetermined number of vanishing moments. When transforms, which are based on splines of higher orders are implemented, it is advisable to switch from time-domain to frequency-domain implementation [7] [8]. Then, an increase in the number of vanishing moments and the regularity of wavelets does not affect the computational cost of the implementation.

We analyzed scaling functions and wavelets associated with the devised wavelet transforms. In particular, we established conditions for exponential decay of the scaling functions and determined the rate of decay. We found that the synthesis scaling functions derived from interpolatory polynomial splines of even degrees coincide with fundamental splines.

We explored the applicability of the newly designed transforms to still image compression. The performance (quality and computational cost) of the presented transforms proved to be comparable with the 9/7 transform. Most of the filters that are employed in the transforms are IIR. They are also applicable to the design of new subdivision schemes [49] and framelet transforms [12].

In the future we intend to find accurate estimates of smoothness (Hölder exponents) of the designed scaling functions and wavelets. We plan to extend our technique to the irregularly sampled signals.

Acknowledgement:

This research was partially supported by the grant, *Construction of spline based filter banks for the wavelet analysis and image processing application,* of Tel Aviv University.

References

References

1. M. Abramovitz and I. Stegun, *Handbook of mathematical functions*, (Dover Publ. Inc., New York 1972).
2. J. H. Ahlberg, E. N. Nilson and J. L. Walsh, *The theory of splines and their applications*, (Acad. Press, New York, 1967).
3. A. Aldroubi, M. Eden and M. Unser, Discrete spline filters for multiresolutions and Wavelets of l_2, *SIAM Math. Anal.,* **25**, (1994), 1412-1432.
4. M. Antonini, M. Barlaud, P. Mathieu and I. Daubechies, Image coding using wavelet transform, *IEEE Transaction on Image Processing,* **1**(2) (1992),205-220.
5. A. Z. Averbuch, F. G. Meyer, J.-O. Strömberg, Fast adaptive wavelet packet image compression, *IEEE Trans. on Image Processing,* **9**(5), (2000), 792-800.
6. A. Z. Averbuch, A. B. Pevnyi and V. A. Zheludev Butterworth wavelet transforms derived from discrete interpolatory splines: Recursive implementation, *Signal Processing*, **81**, (2001), 2363-2382.
7. A. Z. Averbuch, A. B. Pevnyi and V. A. Zheludev, Biorthogonal Butterworth wavelets derived from discrete interpolatory splines, *IEEE Trans. Sign. Proc.,* **49**, No.11,(2001), 2682-2692.
8. A. Averbuch and V. Zheludev, Construction of biorthogonal discrete wavelet transforms using interpolatory splines, *Applied and Comp. Harmonic Analysis,* **12** (2002), 25-56.
9. A. Averbuch and V. Zheludev, Splines: a new contribution to wavelet analysis, Proc. Conference Algorithms for Approximation IV, Huddersfield, 2002.
10. A. Z. Averbuch, V. A. Zheludev, A new family of spline-based biorthogonal wavelet transforms and their application to image compression, *IEEE Trans. on Image Proc.,* vol. 13, no. 7, (2004), 993-1007.
11. G. Battle, A block spin construction of ondelettes. Part I. Lemarié functions, *Comm. Math. Phys.* **110** (1987), 601-615.
12. A. Z. Averbuch, V. A. Zheludev and T. Cohen Interpolatory frames in signal space, to appear in *IEEE Trans. Signal Processing.*
13. C. K. Chui and J. Z. Wang, On compactly supported spline wavelets and a duality principle, *Trans. Amer. Math. Soc.* **330**(1992), 903-915.
14. A. Cohen, I. Daubechies and J.-C. Feauveau, Biorthogonal bases of compactly supported wavelets, *Commun. on Pure and Appl. Math.* **45** (1992), 485-560.
15. A. Cohen and I. Daubechies, A new technique to estimate the regularity of refinable functions, *Revista Matematica Iberoamericana,* **12** (1996), 527–591.
16. I. Daubechies, *Ten lectures on wavelets*, (SIAM. Philadelphia, PA, 1992).
17. I. Daubechies and Y. Huang, A decay theorem for refinable functions, *Applied Mathematics Letters,* **7**, (1994), 1–4.
18. I. Daubechies, and W. Sweldens, Factoring wavelet transforms into lifting steps, *J. Fourier Anal. Appl.*, **4** (1998) 247–269.
19. G. Deslauriers and S. Dubuc, Interpolation dyadique. In *Fractals, Dimensions nonentières et applications.* Paris: Masson, 1987.
20. G. Deslauriers and S. Dubuc, Symmetric iterative interpolation processes, *Constructive Approximation,* **5** (1989), 49-68.
21. D. L. Donoho, Interpolating wavelet transform, Preprint 408, Department of Statistics, Stanford University, 1992.
22. N. Dyn, J. A. Gregory and D. Levin, Analysis of uniform binary subdivision schemes for curve design, *Constr. Approx.*, **7** (1991), 127–147.

23. N. Dyn, Analysis of convergence and smoothness by the formalism of Laurent polynomials, in Tutorials on Multiresolution in Geometric Modelling, A. Iske, E. Quak, M.S. Floater, eds., Springer 2002, 51-68.
24. G. Fix and G. Strang, Fourier analysis of the finite element method in Ritz-Galerkin theory, *Stud. Appl. Math.*, **48** (1969), 265-273.
25. C. Herley and M. Vetterli, Wavelets and recursive filter banks, IEEE Trans. Signal Proc., **41(12)** (1993), 2536-2556.
26. P.G. Lemarié, Ondelettes à localization exponentielle, *J. de Math. Pures et Appl.* **67**(1988), 227-236.
27. D. Marpe, G. Heising, A. P. Petukhov, and H. L. Cycon, Video coding using a bilinear image warping motion model and wavelet-based residual coding, Proc. SPIE Conf. on Wavelet Applications in Signal and Image Processing VII, Denver, CO, July 1999, SPIE, Vol. 3813, pp. 401 – 408.
28. A. V. Oppenheim and R. W. Shafer, *Discrete-time signal processing*, (Englewood Cliffs, New York, Prentice Hall, 1989).
29. A. B. Pevnyi and V. A. Zheludev, On the interpolation by discrete splines with equidistant nodes, *J. Appr. Th.,* **102** (2000), 286-301.
30. A. P. Petukhov, Periodic wavelets, *Sb. Math.* **188**(10) (1997), 1481–1506.
31. A. P. Petukhov, Biorthogonal wavelet bases with rational masks and their applications, *Proc. of St. Petersburg Math. Soc., 7* (1999), 168 – 193. (Russian)
32. A. B. Pevnyi and V. A. Zheludev, Construction of wavelet analysis in the space of discrete splines using Zak transform, *J. Fourier Analysis and Application,* **8**(1), (2002) 55-77.
33. N. Saito and G. Beylkin, Multiresolution representations using the auto-correlation functions of compactly supported wavelets, *IEEE Trans. Signal Proc.,* **41**(12), (1993), 3594-3590.
34. G. Strang, and T. Nguen, Wavelets and filter banks, Wellesley-Cambridge Press, 1996.
35. I. J. Schoenberg, Contribution to the problem of approximation of equidistant data by analytic functions, *Quart. Appl. Math.* **4** (1946), 45-99, 112-141.
36. I. J. Schoenberg, On spline functions, In *Inequalities*, (O. Shisha ed.) (1967), 255-291.
37. I. J. Schoenberg , Cardinal interpolation and spline functions, *J. Approx. Th.,* **2**, (1969), 167-206.
38. I. J. Schoenberg, Cardinal interpolation and spline functions II, Interpolation of data of power growth, *J. Approx. Th.,* **6**, (1972), 404-420.
39. L. L. Schumaker, Spline functions: Basic theory, Wiley, 1981.
40. Yu. N. Subbotin, On the relation between finite differences and the corresponding derivatives, *Proc.Steklov Inst. Math.* **78** (1965), 24-42.
41. W. Sweldens The lifting scheme: A custom design construction of biorthogonal wavelets, *Appl. Comput. Harm. Anal.* **3(2)**, (1996), 186-200.
42. M. Unser, A. Aldroubi and M. Eden, B-spline signal processing: Part I–theory, *IEEE Trans. Signal Process,* **41**(2) (1993), 821-832.
43. M. Unser, A. Aldroubi and M. Eden, B-spline signal processing: Part II–Efficient design and applications, *IEEE Trans. Signal Process*, **41**(2) (1993), 834-848.
44. M. Unser, A. Aldroubi and M. Eden, A family of polynomial spline wavelet transforms, *Signal Processing,* **30**, (1993), 141-162.
45. V. A. Zheludev, Periodic splines and the fast Fourier transform, *Comput. Math. & Math. Phys.,* **32**(2) (1992), 149-165.
46. V. A. Zheludev, Local spline approximation on a uniform grid, *U.S.S.R. Comput. Math. & Math. Phys.*, **27**(5) (1987), 8-19.

47. V.A. Zheludev, Local smoothing splines with a regularizing parameter, *Comput. Math. & Math Phys.*, **31**, (1991), 193-211.
48. V. A. Zheludev, Periodic splines, harmonic analysis, and wavelets. In *Signal and image representation in combined spaces*, 477–509, Wavelet Anal. Appl., 7," (eds. Y. Y. Zeevi and R. Coifman), Academic Press, San Diego, CA, 1998.
49. V. A. Zheludev, Interpolatory subdivision schemes with infinite masks originated from splines, to appear in *Advances in Comp. Math.*